

Review

Phase Diagrams for Systems Containing Hyperbranched Polymers

Sabine Enders ^{1,*}, Kai Langenbach ¹, Philipp Schrader ¹ and Tim Zeiner ²

- ¹ TU Berlin, Fachgebiet Thermodynamik und Thermische Verfahrenstechnik, Sekr. BH 7-1, Ernst-Reuter-Platz 1, D-10587 Berlin, Germany; E-Mails: Kai.Langenbach@tu-berlin.de (K.L.); p.schrader@tu-berlin.de (P.S.)
- ² TU Dortmund, Lehrstuhl Fluidverfahrenstechnik, Emil-Figge-Str. 70, D-44227 Dortmund, Germany; E-Mail: Tim.Zeiner@bci.tu-dortmund.de
- * Author to whom correspondence should be addressed; E-Mail: Sabine.Enders@tu-berlin.de; Tel.: +49-30-314-227-55; Fax: +49-30-314-224-06.

Received: 2 November 2011; in revised form: 15 December 2011 / Accepted: 4 January 2012 / Published: 9 January 2012

Abstract: Hyperbranched polymers show an outstanding potential for applications ranging from chemistry over nanotechnology to pharmacy. In order to take advantage of this potential, the underlying phase behaviour must be known. From the thermodynamic point of view, the modelling of these phase diagrams is quite challenging, because the thermodynamic properties depend on the architecture of the hyperbranched polymer as well as on the number and kind of present functional end groups. The influence of architecture can be taken into account via the lattice cluster theory (LCT) as an extension of the well-known Flory-Huggins theory. Whereas the Flory-Huggins theory is limited to linear polymer chains, the LCT can be applied to an arbitrary chain architecture. The number and the kind of functional groups can be handled via the Wertheim perturbation theory, applicable for directed forces between the functional groups and the surrounding solvent molecules. The combination of the LCT and the Wertheim theory can be established for the modelling or even prediction of the liquid-liquid equilibria (LLE) of polymer solutions in a single solvent or in a solvent mixture or polymer blends, where the polymer can have an arbitrary structure. The applied theory predicts large demixing regions for mixtures of linear polymers and hyperbranched polymers, as well as for mixtures made from two hyperbranched polymers. The introduction of empty lattice sites permits the theoretical investigation of pressure effects on phase behaviour. The calculated phase diagrams were compared with own experimental data or to experimental data taken from literature.

Keywords: lattice cluster theory; Wertheim lattice theory; hyperbranched polymer; phase equilibria; miscibility

Symbols

b	Number of branching points
С	Contributions to the Helmholtz energy within the lattice cluster theory
D	Corrections to the Flory-Huggins theory, connectivity factor (Equation (20))
Е	Internal energy
F	Helmholtz energy
f	Mayer functions
G	Gibbs energy
g	Generation number
Н	Enthalpy or summands in Equation (37)
I, J	Summands in Equation (38)
J	Grand thermodynamic potential
K, L, M	Factors describing the architecture of the polymer, defined in Equations (78,79)
Κ	Ratio of nearest-neighbour positions with a proper orientation to all possible orientations
k	Interaction parameter (Equation (91))
М	Molecular weight or number of segments
m	Number of chains in the system
Ν	Topological coefficient (Table 1) or number of lattice sites
n	Amount of mole
Р	Pressure
р	Counting variable
Q	Summands in Equation (41)
r	Position of the segments
S	Entropy
Т	Temperature
u	Interaction potential
V	Volume
V	Specific volume
W	Microcanonical partition function
W	Mass fraction
Х	Mole fraction
Ζ	Partition function
Z	Coordination number

Polymers **2012**, *4*

Superscript

a, b	Phase a or b
ath	Athermic mixture
LV	Liquid-vapour equilibrium
MF	Mean field approach
reg	Regular mean field energetic contribution

Subscript

A_i	Non-bonded segment to the association site A
asso	Association
att	Attractive part of the interaction potential
В	Boltzmann constant
СН	Solvent cyclohexane
comp	Pure compound
FH	Flory–Huggins theory
i	Component i or counting variable
1	Lattice
LCT	Lattice cluster theory
Polymer	Polymer
R	Repulsive part of the interaction potential
V	Void lattice site

Creek letters

χ	Flory–Huggins interaction parameter
α	Factor in the polynomial series in Equation (29)
β	Vector pointing to the next neighbour
Δ	Difference or association strength
δ	Kronecker Delta function
ε	Interaction energy
ϕ	Volume fraction
Φ	Segment molar fraction
γ	Corrections to the Flory–Huggins theory, combinatorial factor (Equation (20))
К	Association volume in the original Wertheim theory
μ	Chemical potential
ρ	Density

 σ Length of a cubic cell

1. Introduction

Changing the polymer architecture from that of conventional linear to partially or highly branched is one of the methods available to tailor a material's properties for a specific application where high performance or a specific functionality is required. Highly branched polymers are dendritic polymers, including dendrimers with a perfectly branched, monodisperse structure, imperfectly branched polymers, or hyperbranched polymers (HBP). These advanced materials are gaining more and more interest in recent years because of their tailor-made properties. Due to their architecture, HBP show a lower viscosity in melt and solution compared to their linear analogue and the rich amount of various functional groups offers a tuneable solubility in different solvents. Based on these advantages of HBP different applications have been suggested, for instance possible implementations of HBP are discussed in the field of medicine [1-8], catalysis [9-13], membrane materials [14-20], chemical engineering [21–24], sensors [25–28], thermosets [29–31] or as rheological modifier [32,33]. Polymeric drug delivery systems offer great opportunities to effectively control the drug release in human body [34–44]. In addition dendrimers can be surface engineered to release the drug at desired site, that is, as targeted drug delivery. This property along with the solubilisation behaviour could improve the bioavailability of drugs [45–47]. Several recently published reviews informed about the functions and applications of dendrimers resulting from supramolecular and physical properties can be found in the literature [48–51].

However, one should recognize that the break-through in terms of industrial application is still a promising vision with few exceptions. At present, an exact determination of the structure and molar mass characteristics of hyperbranched polymers using available characterization techniques is not completely feasible (e.g., [52]) and hence, the detailed description of the physical properties is challenging. This is especially true for the involved phase equilibria. Recently [53–58], large strides have been made in understanding and developing theories for the thermodynamic properties of hyperbranched polymers, but an accurate prediction of the phase behaviour of these complex systems is still very much in its infancy. The question arising in calculating the phase equilibria of HBP is the consideration of branching effects. Kleintjens et al. [59] showed for the system polyethylene + diphenyl ether that the two-phase region of a branched polyethylene solution may be shifted by more than 10 °C compared to that of a linear polyethylene sample of about equal number and mass average molar mass. Additionally, de Loos et al. [60] measured high pressure phase equilibria of branched polyethylene + ethylene and linear polyethylene + ethylene. They figured out that there are significant differences in the cloud point pressure. Vapour pressure measurements for polymer solutions made from polyisoprene (linear and branched) and cyclohexane, performed by Eckelt et al. [61], demonstrates the influence of the degree of branching on the solution properties. According to these results [59-61] it can be stated that the calculation of phase equilibria of branched polymers needs the consideration of polymer architecture in the thermodynamic equations.

Polymer theory has started to deal with the effects of different molecular architectures of polymer a long time ago [62–67] and this research field retains its attraction. In literature there are several possibilities proposed to calculate the phase behaviour of HBP. One way is the UNIFAC-FV (Universal Quasichemical Functional Group Activity Coefficients-Free Volume) approach, which is proposed by Seiler [68] and Kouskoumvekaki *et al.* [69]. The UNIFAC-FV [70] is a method to

estimate solvent activities of polymer solutions. The approach is based on a group contribution method (*i.e.*, UNIFAC [71]) in combination with a free volume correction. Seiler [68] pointed out that with the help of the UNIFAC-FV model the vapour-liquid phase equilibria (VLE) of hyperbranched polymer solution could be described in a proper manner. But the occurrence of liquid-liquid phase equilibria (LLE) of hyperbranched polymer solution cannot be predicted by the UNIFAC-FV model. Hyperbranched polymers are distinguished from linear polymers by their architecture, but this issue cannot be taken into account by the UNIFAC-FV. The activity coefficient of the polymer, unlike that of the solvents, depends strongly on the branching degree. In LLE both activity coefficients are essential, whereas in VLE only the one of the solvent plays an important role. Therefore, UNIFAC models the VLE successfully, but not the LLE. Another possibility to calculate phase equilibria is offered by the PC-SAFT (Perturbed Chain-Statistical Association theory) equation of state. The physical foundation of the SAFT (Statistical Association Fluid Theory)-family equations of state [72] was built up by Wertheim applying perturbation theory of first and second order for directional interactions [73-76]. Chapman et al. [77] extended the formalism to mixtures and developed an engineering approach for the description of associating fluids. Gross and Sadowski [78] introduced an interaction potential with soft repulsion and called this equation of state PC-SAFT. For modelling hyperbranched polymers, PC-SAFT was applied with extensions accounting for dipolar and quadrupolar interactions and a branching term describing the architecture of hyperbranched polymers [79,80], coarsely. Kozłowska et al. [79] calculated the VLE in good agreement with experimental results: however, the occurrence of the miscibility gap could not be predicted. One objection to the branching term is the fact that all branching points have four bonds, but the majority number of branching points of hyperbranched polymers has three bonds: therefore, this branching term fails to describe the architecture of hyperbranched polymers correctly. To the best of our knowledge, only the detailed incorporation of the architecture allows the modelling of the LLE close to experimental data [53–58].

The classical way of describing the phase behaviour of polymer containing systems [81–83] is the Flory-Huggins (FH) theory [84-86]. In the framework of FH theory, individual monomers are treated as single entities, devoid of any chemical structure. Flory and Huggins [84] employed a very simple mean-field approximation that essentially ignores the details of the polymer chain connectivity and, therefore, cannot distinguish between linear, star, branched, and comb polymer architecture. In order to overcome these deficits, Freed and coworkers [87–92] developed the lattice cluster theory (LCT), which extends the FH theory. In 1991, Dudowicz and Freed [89–91] have developed a systematic expansion of the partition function of a lattice polymer using the LCT. This model takes into account the effect of branching on the thermodynamic properties of polymer blends. Jang and Bae [93] have used the LCT to model LLE of an aqueous hyperbranched polymer solution for the first time, but they were not able to describe the liquid-liquid phase behaviour of hyperbranched polymer solution in accordance with experimental data. In a later work, Jang and Bae [94] have included in addition to the LCT also a term describing the self-association of water. Using this model they could compute the phase equilibrium in agreement with experimental data. They concluded that the self-association of water is the main influence on the liquid phase behaviour. However, the problems arising in the application of the LCT goes back to incorrectness in the used equation [53]. Sometimes a simplified version of the LCT is used [95,96]. Comparing all presented theories, only the LCT is able to describe the influence of the polymer architecture on the phase equilibrium of hyperbranched polymer

solutions. For these reasons the LCT will be examined in the following sections to investigate phase equilibria of HBP solutions.

In addition to the architecture, the present functional groups also have an influence on polymer phase behaviour. Moorefield and Newkome [97] showed that dendrimers with very hydrophobic interiors such as polyethers and polycarbosilanes can be made water soluble by introducing hydrophilic functional groups. In contrast to this, water soluble dendrimers can be made hydrophobic by converting their functional groups into hydrophobic units [97]. For these reasons, the influence of functional groups on phase behaviour has to be regarded. We focus our attention to HBP with polar functional groups which are able to contribute to association forces. In principal, there are two different ways of describing association between different molecules in literature [98]. One possibility is to treat the forming of hydrogen bonds as chemical reactions and this approach is called the "chemical" theory. Another way is the "physical" theory, based on the solution of integral equations including potential functions, which describe the association interaction. In the case of hyperbranched polymers both approaches can be used [57]. In this contribution a physical association theory, developed by Wertheim [73–76] is utilized to model the influence of polar functional groups of the HBP and of the polar solvent on the phase equilibrium.

2. Theory

The well-established way of dealing with phase equilibria including polymers is the FH theory, which was developed by Flory and Huggins [84,86].

While the FH model describes successfully the fact of immiscibility of long chain polymers in solution, other aspects can only be described qualitatively. In order to improve the FH theory, Freed and co-workers [87–91] have developed perturbative methods for systematically calculating corrections to the FH theory. This theory emerges in the form of a cluster expansion, similar to Mayer cluster expansion [99] for non-ideal gases, and is called the lattice cluster theory (LCT). This theory will be presented in an incompressible and compressible version. Both theories, the FH theory and the LCT, have one deficit in common: They cannot describe the hydrogen bonding of associating components. One possibility to include this kind of interaction is the thermodynamic perturbation theory of first or second order developed by Wertheim [73–76]. These theories will be presented in this section, but at first a short introduction to phase equilibrium thermodynamics will be presented.

2.1. Phase Equilibrium Thermodynamics

Phase equilibria such as VLE or LLE do play an important role in separation processes as well as in drug delivery or other pharmaceutical applications. As this section is concerned with the thermodynamic phase behaviour of HBP the main focus lies on the thermodynamic description of LLE.

2.1.1. Ensembles and Potentials

LLE often occur, when species are mixed differing strongly in either polarity or molar mass or both. Typical examples are mixtures of a non-polar alkane (e.g., octane) and the highly polar water [100] or mixtures of a long chain polymer (e.g., polyethylene) and a small chain alkane (e.g., hexane) [101]. In

phase equilibrium thermodynamics the usual approach to describe phase behaviour is the mean field approach. Using this method the many body problem of describing the kinetic and potential energy of each molecule in a mixture is approximated, mostly using statistical mechanics [102]. The result after the choice of a statistical ensemble is one of three thermodynamic potentials, depending on their respective natural observables [103].

The thermodynamic potentials are entropy:

$$S(E,V,n_i) \tag{1}$$

Helmholtz free energy:

$$F(T,V,n_i) \tag{2}$$

and the grand thermodynamic potential

$$J(T,V,\mu_i) \tag{3}$$

The observables are internal energy E, volume V, temperature T, amount of substance i, n_i , and the chemical potentials of the components i, μ_i . The derivatives of the respective potentials, with respect to their natural variables, yield all other thermodynamic information. For example the derivative of Helmholtz energy with respect to volume results in the negative system pressure, -P:

$$\left(\frac{\partial F}{\partial V}\right)_{T,n_i} = -P \tag{4}$$

It is possible to transform between these potentials with the Legendre transformation. Thereby, one observable is replaced by another in the following way:

$$\Xi\left(\frac{\partial\Psi}{\partial\tau},\ldots\right) = \Psi\left(\tau\left(\frac{\partial\Psi}{\partial\tau}\right),\ldots\right) - \frac{\partial\Psi}{\partial\tau}\tau\tag{5}$$

Here Ξ and Ψ are the respective potentials and τ is one of the natural variables of potential, Ψ . The list of common transformations is shown below.

$$E(S,V,n_i) = H - PV \tag{6}$$

$$F(T,V,n_i) = E - TS \tag{7}$$

$$G(T, P, n_i) = F + PV \tag{8}$$

$$H(S, P, n_i) = G + TS \tag{9}$$

Here entropy and energy change their roles as potential and observable. The potentials are: internal energy E, Helmholtz free energy F, Gibbs energy G and enthalpy H.

2.1.2. Phase Equilibrium Calculations

In calculations of equilibria between two separated phases a and b the Helmholtz free energy F and the Gibbs energy G are of substantial importance. Both these potentials do have a minimum in equilibrium. This means, an optimization approach to the calculation of equilibria is feasible.

$$G \to \min \tag{10}$$

subject to
$$T^a = T^b$$
 and $P^a = P^b$ (10)

$$F \to \min$$

subject to $T^{a} = T^{b}$ and $P^{a}(V^{a}) = P^{b}(V^{b})$ (11)

The Gibbs energy minimization, on the one hand, is typically used for phase separations, where pressure does not play a crucial role or is accorded for otherwise. The Helmholtz free energy minimization, on the other hand, is used when compressibility of the system is of concern. In both cases the condition of chemical equilibrium ensues:

$$\mu_i^a = \mu_i^b \tag{12}$$

In case of Helmholtz free energy the optimization yields the additional condition of mechanical equilibrium. This condition is trivial for the Gibbs energy, because it depends directly on the pressure and not on the volume.

$$P^{a}\left(V^{a}\right) = P^{b}\left(V^{b}\right) = P \tag{13}$$

The equilibrium can be calculated using Equations (12) and (13). This solution ensures that the condition of thermal equilibrium

$$T^a = T^b = T \tag{14}$$

is also fulfilled. Hence, the problem to solve is a (typically nonlinear) system of equations with k equations or k+2 equations for a compressible system, where k is the number of components.

2.1.3. Flory–Huggins Theory

In polymer thermodynamics one is challenged with the immanent huge difference in molar mass between the solute and the solvent. This generally leads to the fact that molar based approaches to calculate the phase behaviour of polymers in solution are predetermined to fail. This can be understood, if the limiting case of infinite molar mass $M \to \infty$ is examined. Here, the mole fraction of the polymer approaches zero implying that Raoult's law [104] is applicable for the solvent, yet the mixture is highly non-ideal. Figure 1 demonstrates an impressive example, namely the vapour pressure of a polymer solution. According to Raoult's law, the vapour pressure of the considered solution should change linearly (straight line in Figure 1) from the vapour pressure of the solvent to zero pressure, because the vapour pressure of the pure polymer is zero. However, the experimental data, taken from the literature [61], are far away from Raoult's law. Additionally, the experimental data in Figure 1 clearly shows the impact of polymer architecture on the thermodynamic properties. Although the same type of polymer from the chemical point of view (linear and branched polyisoprene) in the same solvent (cyclohexane) was used, differences in the vapour pressure are found experimentally. These differences can only be explained by the influence of the chain architecture on the thermodynamic properties. The experimental results demonstrate that cyclohexane is a considerably worse solvent for branched polyisoprene than for the linear analog at all temperatures and at all compositions. This finding is in seeming contrast to the widespread notion that branched polymers are better soluble than their linear counterparts. It may, however, well be that special interactions between

the components of the mixture and larger differences between the end groups and the middle groups of the polymer are capable to change the picture.

Figure 1. Vapour Pressure of polymer solutions P^{LV} , divided by the vapour pressure of the pure solvent P_{CH}^{LV} , made from linear (black symbols) or branched (blue symbols) polyisoprene and cyclohexane [61].

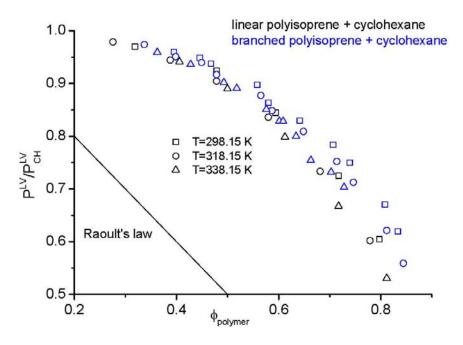
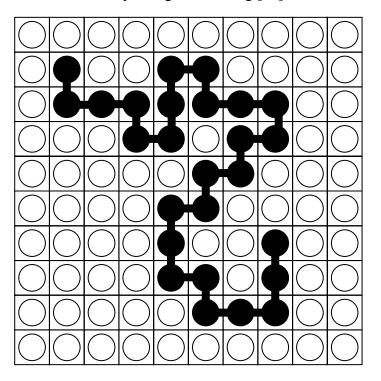


Figure 2. Random walk of a polymer chain in solute on a two dimensional lattice with coordination number four after Flory's original drawing [84].



Flory [84] suggested a way to describe polymer chain solutions avoiding this complication. For this purpose he introduced a lattice on which the solvent occupies a single lattice site and the polymer may

occupy several neighbouring lattice sites, as depicted in Figure 2. In order to calculate the micro-canonical partition function W of a system containing a solvent and a linear polymer, the number of ways to consecutively insert a polymer chain into a lattice of coordination number z, at first fully occupied by solvent beads, must be calculated.

This is done by Flory [84], by assuming that

- (a) a polymer chain is composed of M segments of equal size.
- (b) the polymer segments size equals that of the solvent.
- (c) the polymer is inserted randomly, but can fill the lattice completely (*i.e.*, forms a perfect crystal).

From this he derived the athermal entropy of mixing per lattice site [84]:

$$\frac{\Delta S_{FH}^{ath}}{N_l k_B} = \frac{\Phi_1}{M_1} \ln \Phi_1 + \frac{\Phi_2}{M_2} \ln \Phi_2$$
(15)

Here N_i is the number of lattice sites, k_B is the Boltzmann constant, M_2 is the number of segments the polymer is composed of, $M_1 = 1$ is the number of solvent segments, and the Φ_i are the segment mole fractions of components *i*, defined as:

$$\Phi_i = \frac{M_i n_i}{\sum M_j n_j} \tag{16}$$

In addition a regular mean field energetic contribution of the molecules on the fully occupied lattice is introduced [84]:

$$\frac{\Delta \mathcal{E}_{FH}^{reg}}{N_l k_B T} = \frac{z \Delta \mathcal{E}_{12}}{2k_B T} \Phi_1 \Phi_2 = \frac{z \left(\mathcal{E}_{11} + \mathcal{E}_{22} - 2\mathcal{E}_{12}\right)}{2k_B T} \Phi_1 \Phi_2 = \chi \Phi_1 \Phi_2 \tag{17}$$

Usually the interaction energy is expressed in terms of $\chi = \frac{z\Delta \varepsilon_{12}}{2k_B T}$. By using Equation (7) the

Helmholtz free energy is derived [84].

$$\frac{\Delta F_{FH}}{N_l k_B T} = -\frac{\Phi_1}{M_1} \ln \Phi_1 - \frac{\Phi_2}{M_2} \ln \Phi_2 + \chi \Phi_1 \Phi_2$$
(18)

Though the FH theory is useful for calculating LLE of simple chain polymers, it does neglect the structure of the molecules completely. However, in order to achieve quantitative agreement with experimental data, a concentration-dependent interaction parameter χ was introduced [81–84]. The approach, employed to calculate the phase behaviour of hyperbranched polymers, is the extension of FH theory based on physical argumentation.

2.2. Lattice Cluster Theory

In 1985 Freed [105] reawakened the idea of de Gennes [106] and des Cloizeaux [107], treating polymer solutions as a self-avoiding walk on a lattice by introducing n-component spins on each lattice side. It was shown that by reducing this lattice theory to the mean field approximation of lowest order the FH theory was obtained [87]. This situation allows the calculation of corrections [87,88] to the mean field approach of Flory [84] and Huggins [86], but these corrections did not consider the influence of interactions between the segments on the arrangement of segments on the lattice. Firstly,

the interactions have been considered by Pesci *et al.* [108]. Dudowicz *et al.* [89–91] derived the LCT in an analytical way and introduced the influence of polymer architecture. A detailed paper about the state of the art can be found in the literature [109].

2.2.1. LCT of Incompressible Systems

As the LCT is an extension of the FH theory, both theories have the same fundamental idea of a lattice, which is occupied by a polymer and so the polymer can be divided in different segments. Using this idea, the exact partition function of a polymer blend where two segments *i* and *j* interacts with the energy ε_{ii} can be read as [92]:

$$Z = \prod_{\mu=1}^{k} \frac{1}{n_{\mu}! 2^{n_{\mu}}} \sum_{\substack{i_{1,1}^{l} \neq i_{2,1}^{l} \neq i_{3,1}^{l} \neq \dots \neq i_{N_{1},1}^{l} \\ \neq i_{1,2}^{l} \neq i_{2,2}^{l} \neq \dots \neq i_{N_{1},2}^{l}} \prod_{m_{\mu}=1}^{n_{\mu}} \left\{ \prod_{\alpha_{\mu}=1}^{N_{\mu}-1} \sum_{\beta_{\alpha,m}^{\mu}=1}^{z} \delta(i_{\alpha,m}^{\mu}, i_{\alpha+1,m}^{\mu} + \beta_{\alpha,m}^{\mu}) \right\} \exp\left(\sum_{\mu=1}^{k} \sum_{\lambda \leq \mu} \sum_{i_{\mu} \neq j_{\lambda}} \varepsilon_{\mu\lambda}^{ij} \right)$$

$$\cdots$$

$$= i_{1,m}^{l} \neq i_{2,m}^{l} \neq \dots \neq i_{N_{1},m}^{l}} \prod_{m_{\mu}=1}^{m_{\mu}} \left\{ \prod_{\alpha_{\mu}=1}^{N_{\mu}-1} \sum_{\beta_{\alpha,m}^{\mu}=1}^{z} \delta(i_{\alpha,m}^{\mu}, i_{\alpha+1,m}^{\mu} + \beta_{\alpha,m}^{\mu}) \right\} \exp\left(\sum_{\mu=1}^{k} \sum_{\lambda \leq \mu} \sum_{i_{\mu} \neq j_{\lambda}} \varepsilon_{\mu\lambda}^{ij} \right)$$

$$(19)$$

where δ is the Kronecker delta function and the vector β is pointed from a given lattice site to the *z* nearest neighbour lattice sites. A factor n_{μ} ! has to be introduced for the indistinguishability of polymer chains of the same species μ and the factor $\frac{1}{2}$ accounts for the symmetry of each chain. The outside summation in Equation (19) prohibits any lattice site from being occupied by two polymer segments. In the outside summation of Equation (19) there are two factors, whereas the first factor accounts for the bonding constraints in the polymer, the second factor describes the Van der Waals interaction between two lattice sites. The expression in Equation (19) represents an exact solution of a *k* component polymer blend on a cubic Bravais lattice, but for using this approach a simplification is desirable. In the FH theory this simplification is the assumption that just the next neighbours of one polymer segment have to be considered. Freed and Dudowicz [89] extend the assumption of the FH theory by the introduction of a cluster expansion. This expansion goes back to the cluster expansion introduced by Mayer [99] for non-ideal gases. In the framework of LCT, the corrections to the Helmholtz free energy are derived in form of a cluster series expansion in the inverse coordination number 1/z and in the reduced interaction energy $\varepsilon_{\mu\nu}/k_BT$, taking into account the growing correlations between near segments on the same molecule.

By introducing these cluster expansions and fundamental statistical thermodynamics, the Helmholtz free energy of a k component polymer blend reads as [89]:

$$\frac{F}{k_B T} = -\ln\left(W^{MF}\right) - N_l \frac{z}{2} \sum_{\lambda=1}^k \sum_{\mu=1}^k \varepsilon_{\lambda\mu} \Phi_{\lambda} \Phi_{\mu} - \sum_{B,l} \left[\gamma_{D,l} D_{B,l}\right]^C$$
(20)

where the first two terms in Equation (20) are the mean field contributions to the entropy and the interaction energy of the Helmholtz free energy. The third term of Equation (20) represents the corrections to the mean field approach of the FH theory. It appears in form of a cumulant cluster diagram, which has to be evaluated for different orders of the interaction energy. Usually, the evaluation is truncated at the second order of the reduced interaction energy $\varepsilon_{\mu\nu}/k_BT$ as suggested by Freed and Dudowicz [89]. One example of evaluating the second order contribution such a diagram will be shown in the following.

$$\begin{pmatrix} \bullet & \times & \times \\ \bullet & \times & \times \\ \bullet & \times & \times \end{pmatrix}$$
 (C) (21)

In term (21) there is a cumulant cluster diagram of three bonded monomers (solid circles with solid line) and two pairs of interacting monomers (stars with dotted lines). The solid lines represent covalent bonds and the dotted lines physical interaction energies. The monomers in this cumulant cluster diagram do not belong to the trimer chain. To evaluate this diagram, it has to be expanded in a series as shown by Dudowicz and Freed [89].

In Equation (22) the cumulant cluster diagram is expanded in four diagrams. Two of these diagrams in Equation (22) are vanishing in the thermodynamic limit. The other diagrams have to be evaluated. The analysis of these diagrams needs the knowledge of two factors. One factor is the combinatorial factor γ_D , which depends on the number of components and is independent of the polymer architecture. As an example the diagram k1 in Equation (22) is evaluated. For a one component system it is obtained:

$$\gamma_D = \frac{N_2 M^4 m (m-1)(m-2)(m-3)(m-4)}{5!}$$
(23)

where N_2 and M are the number of two successive bonds in a single polymer chain and in that order the number of monomers of one chain, while m is the number of chains in the system. The factor 1/5! arises because of the indistinguishability of selecting the chains.

This formalism can be extended to a multi-component system by labelling all monomers in the diagram. In the case with only distinct labels the factor of indistinguishability reduces to unity. The other factor which has to be evaluated is the connectivity factor for each diagram with B bonds [89]:

$$D_{B} = \alpha d_{B} \tag{24}$$

where α depends only on the number of lattice sites N_l and the number of vertices in the diagram N_v [89]. The factor d_B depends only on the lattice, but not on the polymer architecture. The evaluation process is shown by Dudowicz and Freed [89]. By knowledge of the combinatorial factor and the connectivity factor, this diagram can be analysed. The evaluation leads to the contribution [89]:

$$C_{23} = 3\sum_{i} N(2,i) \sum_{j} \sum_{k} \sum_{l} \varepsilon_{ij} \varepsilon_{kl} \phi_{i} \phi_{j} \phi_{k} \phi_{l}$$
(25)

Here the segment fraction ϕ_i is that of the compressible mixture:

$$\phi_i = \frac{N_i M_i}{N_v + \sum_j N_j M_j} \tag{26}$$

This segment fraction reduces to the one of the incompressible mixture, if the number of void lattice sites goes to zero, resulting in

$$\Phi_i = \lim_{N_v \to 0} \phi_i = \frac{N_i M_i}{\sum_j N_j M_j}$$
(27)

The evaluation of all cumulant cluster diagrams leads to an expression of the Helmholtz free energy, which will be presented in the following sections.

Lattice Cluster Theory for a Binary Polymer Blend

At first the Helmholtz free energy of an incompressible polymer blend is presented [53,56]. As the polymer blend is regarded as incompressible the three interaction energies can be combined to the single interaction energy (see Equation (17)):

$$\Delta \varepsilon = \varepsilon_{11} + \varepsilon_{22} - 2\varepsilon_{12} \tag{28}$$

The segment molar Helmholtz energy can be calculated as follows:

$$\frac{\Delta F_{LCT}}{N_l k_B T} = \frac{\Phi_1}{M_1} \ln \Phi_1 + \frac{\Phi_2}{M_2} \ln \Phi_2 + \sum_{i=1}^{i=6} \alpha_i \Phi_1^{i}$$
(29)

The first two terms on the right hand side of Equation (29) represent the mean field entropic contribution (see Equation (15)) and M_i is the chain length of component *i*. In Equation (29) the corrections to the FH theory appear in form of a power series. Its coefficients depending only on the polymer architecture, which is described with K_i , L_i , M_i , and the interaction energy $\Delta \varepsilon$ can be computed using the following relations [57]:

$$\alpha_{1} = \frac{z\Delta\varepsilon}{2k_{B}T} - (K_{1}z + K_{3})\frac{\Delta\varepsilon}{zk_{B}T} + \frac{(K_{1} - L_{1})^{2}}{z} - \frac{2(K_{1} - L_{1})}{z^{2}} \Big\{ -K_{3} - 2K_{1}K_{5} + K_{1}^{3}M_{1} - 2L_{1}K_{5} + L_{1}K_{1}^{2}M_{2} - 2L_{1}^{3}M_{1} - 2L_{2} + L_{1}L_{2}M_{2} - L_{3} - 3L_{4} - L_{6} + 4L_{1}L_{5} \Big\}$$

$$+ \frac{2(K_{1} - L_{1})^{2}}{z^{2}} \Big\{ \frac{4}{3}K_{1} + K_{1}^{2} + \frac{8}{3}L_{1} + 2L_{1}K_{1} + 3L_{1}^{2} \Big\} + \frac{(K_{2} - L_{2})^{2}}{z^{2}} \Big\}$$
(30)

$$\begin{aligned} a_{2} &= -\frac{z\lambda\varepsilon}{2k_{b}T} + (2K_{1} - L_{1})\frac{\Delta\varepsilon}{k_{b}T} - \frac{(K_{1} - L_{1})^{2}}{z} + \frac{\Delta\varepsilon}{zk_{b}T} \Big[+ 2K_{3} - 4K_{1}^{2} - 4K_{1}K_{5} + 2K_{1}^{3}M_{1} \\ &+ 10L_{1}K_{1} + 8L_{1}K_{2} + 12L_{1}K_{5} - 2L_{1}K_{1}^{2}(3M_{1} + 2) - 4L_{1}^{2} + 8L_{1}^{2}K_{1} + 2L_{1}^{3}(M_{2} - 2) \\ &+ 2L_{2} - 4L_{2}K_{1} - L_{1}L_{2}M_{2} + L_{3} + 3L_{4} + L_{6} - 4L_{1}L_{3} \Big\} \\ &+ \left(\frac{\Delta\varepsilon}{k_{b}T}\right)^{2} \Big\{ -\frac{z}{4} + 3K_{1} + 3K_{2} + 4K_{5} - K_{1}^{2}(2M_{1} + 1) - \frac{L_{1}}{2} \Big\} \\ &+ \frac{2(K_{1} - L_{1})}{z^{2}} \Big\{ -K_{3} - 4L_{1}K_{5} + 2L_{1}K_{1}^{2}M_{1} + L_{1}^{2}K_{1}M_{2} - 3L_{1}^{3}M_{2} - 2L_{2} + L_{1}L_{2}M_{2} \\ &- L_{3} - 3L_{4} - 2L_{5} - L_{6} + 4L_{1}L_{3} \Big\} - \frac{4(K_{1} - L_{1})^{2}}{z^{2}} \Big\{ 2L_{1} + 3L_{1}^{2}^{2} \Big\} - \frac{(K_{2} - L_{2})^{2}}{z^{2}} \\ &\alpha_{3} = -(K_{1} - L_{1})\frac{\Delta\varepsilon}{k_{b}T} + \frac{\Delta\varepsilon}{zk_{b}T} \Big\{ -K_{5} + 8K_{1}^{2} + 8K_{1}K_{5} - 4K_{1}^{3}(M_{2} + 1) - 16L_{1}K_{1} \\ &- 4L_{1}K_{2} - 12L_{1}K_{5} + 2L_{1}K_{1}^{2}(3M_{1} + 10) + 8L_{1}^{2} + 2L_{1}^{2}K_{1}(M_{2} - 14) \\ &- 4L_{1}^{3}(M_{2} - 3) - 2L_{2} + 4L_{2}K_{1} + L_{1}L_{2}M_{2} - L_{3} - 3L_{4} - L_{6} - 4K_{1}L_{5} + 8L_{1}L_{3} \Big\} \\ &+ \Big(\frac{\Delta\varepsilon}{k_{b}T}\Big)^{2} \Big\{ \frac{z}{2} - \frac{13}{2}K_{1} - 3K_{2} - 6K_{5} + 3K_{1}^{2}(M_{1} + 2) + \frac{5}{2}L_{1} - 6L_{1}K_{1} + 2L_{1}^{2} - L_{2} \Big\} \\ &+ \frac{2(K_{1} - L_{1})}{z^{2}} \Big\{ -2K_{1}K_{5} + K_{1}^{3}M_{1} + 2L_{1}K_{5} - L_{1}K_{1}^{2}M_{1} - L_{1}^{2}K_{1}M_{2} + L_{1}^{3}M_{2} + 2L_{3} \Big\} \\ &+ \frac{8(K_{1} - L_{1})^{2}}{z^{2}} \Big\{ -K_{1} + L_{1} - 3L_{4}K_{1} + 3L_{1}^{2} \Big\} \\ &+ \frac{8(K_{1} - L_{1})^{2}}{z^{2}} \Big\{ -K_{1} + K_{1} - 3L_{4}K_{1} + 3L_{1}^{2} \Big\} \\ &+ \frac{6(K_{2}}}{2} - 2 \Big\} - \frac{2(K_{1} - L_{1})^{4}}{z^{2}} \Big\} \\ &+ \frac{6(K_{2}}}{k_{b}T} \Big]^{2} \Big\{ -\frac{2}{4} + 6K_{1} + K_{2} + 4K_{5} - 2K_{1}^{2}(M_{2} + 6) - 4L_{1} + 18L_{1}K_{1} \\ &+ L_{1}^{2} \Big(\frac{M_{2}}{2} - 7 \Big) + L_{2} - L_{3} \Big\} - \frac{2(K_{1} - L_{1})^{4}}{z^{2}} \Big\} \\ &- L_{1}^{2} \Big(\frac{M_{2}}{2} - 8 \Big) + L_{5} \Big\} \\ &\alpha_{6} = -3 \Big(\frac{\Delta\varepsilon}{k_{b}T} \Big)^{2} \Big(K_{1} - L_{1}^{2} \Big)^{2} \Big(K_{1} - L_{1}^{2} \Big)^{2} \Big(K_{1} - L_{$$

where the corrections made by Dudowicz *et al.* [110] were incorporated. In the limit $z \to \infty$ only the parameters $\alpha_1 = z\varepsilon/(2k_BT)$ and $\alpha_2 = -z\varepsilon/(2k_BT)$ are left, which can be summarized to the well

LCT for a Ternary Polymer Solution

The starting point for the calculation of the Helmholtz free energy of a ternary polymer solution is [56]:

$$\frac{\Delta F_{LCT}}{N_l k_B T} = \frac{\Delta E_1}{N_l k_B T} + \frac{\Delta E_2}{N_l k_B T} - \frac{\Delta S}{N_l k_B}$$
(36)

where the contributions of entropy (ΔS), as well as the first (ΔE_1) and second order (ΔE_2) of energy can be calculated using the tables I, II and III published by Dudowicz and Freed [89] and taking into account the corrections introduced by Dudowicz *et al.* [110]. The entropic part of the Helmholtz free energy reads [56]:

$$\frac{\Delta S}{N_l k_B} = -\frac{\Phi_1}{M_1} \ln(\Phi_1) - \frac{\Phi_2}{M_2} \ln(\Phi_2) - \Phi_3 \ln(\Phi_3) + \sum_{i=1}^7 H_i$$
(37)

where the first terms on the right hand side of Equation (37) represent the contribution to the mean field limit and the following terms are the extensions of the mean field approach. These contributions depend only on the structure of the polymer in terms of K_i , L_i , M_i and they can found in the literature [56].

In addition to the entropic corrections of the LCT, also the energetic corrections to the FH theory have to be determined. The first order mixing energy (ΔE_1) as well as the second order mixing energy (ΔE_2) can be expressed as a sum [56]:

$$\frac{\Delta E_1}{N_l k_B T} = -\sum_{i=1}^{14} I_i; \quad \frac{\Delta E_2}{N_l k_B T} = -\sum_{i=1}^{10} J_i$$
(38)

where the contributions I_i and J_i are given in literature [56]. These contribution depend on the architecture via K_i , L_i , M_i and additionally from the difference in interaction energy of component *i* and *j*, expressed by the three interaction parameters $\Delta \varepsilon_{12}$, $\Delta \varepsilon_{13}$, and $\Delta \varepsilon_{23}$. In the $z \rightarrow \infty$ and $\varepsilon \rightarrow 0$ limit this theoretical framework reduces to the Flory–Huggins expression of a ternary polymer solution and it reduces also correctly to the equation describing a binary mixture (Equation (29)). For applying the LCT, the determination of the architectural parameters is necessary. This will be shown in Section 2.2.3.

2.2.2. LCT of Compressible Systems

For compressible systems the LCT can be extended to account for free volume. The proposal of Freed and co-workers [89–91] is to introduce void lattice sites in order to do that. Void lattice sites are modelled as single sites on the lattice that interact neither with each other nor with other molecules. This leads to a change in the mean field contribution to the partition function:

Polymers 2012, 4

$$W_{comp}^{MF}(n_i, M_i) = \prod_i \frac{1}{n_i! 2^{n_i}} \frac{N_l!}{[N_l - \sum_j M_j n_j]!} \left(\frac{z}{N_l}\right)^{\sum_j (M_j - 1)n_j}$$
(39)

For a pure compound the contributions to the Helmholtz energy per lattice site are as follows:

$$\ln\left(W_{comp}^{MF}\right) = \frac{S_{0i,comp}^{MF}}{N_{l}k_{B}} = -\phi_{v}\ln\phi_{v} - \frac{(1-\phi_{v})}{M_{i}}\left(\ln\left(1-\phi_{v}\right) + \ln\frac{2z}{M_{i}} - M_{i}\ln z + M_{i} - 1\right)$$
(40)

Here ϕ_{ν} is the segment fraction of void lattice cells. The entropic contribution for pure components can be written as a polynomial in the void segment fractions [111,112]:

$$\frac{S_{0i,comp}}{N_l k_B} = \frac{S_{0i,comp}^{MF}}{N_l k_B} + \sum_{p=0}^4 Q_{p,i}^{(s)} \phi_v^p$$
(41)

The coefficients of this polynomial depend on the molecule's structure and on the lattice coordination number z [111,112]:

$$Q_{4,i}^{(s)} = \frac{2}{z^2} \left[N(1,i) \right]^4 \tag{42}$$

$$Q_{3,i}^{(s)} = -\frac{2}{z^2} \left(2N(1,1,i) \left[N(1,i) \right]^2 - \left[N(1,i) \right]^4 M_i + \frac{4}{3} \left[N(1,i) \right]^3 + 4 \left[N(1,i) \right]^4 \right)$$
(43)

$$Q_{2,i}^{(s)} = \frac{1}{z^2} \begin{pmatrix} 2[N(1,i)]^4 (6-3M_i) + 2[N(1,i)]^2 (N(2,i)M_i + 6N(1,1,i)) + [N(2,i)]^2 \\ -2N(1,i) \left(N(3,i) + N(1,2,i) + 3N(\perp,i) + 2N(2,i) - \frac{z}{2}N(1,i) - 4[N(1,i)]^2 \right) \end{pmatrix}$$
(44)

$$\mathcal{Q}_{1,i}^{(s)} = -\frac{1}{z^2} \begin{pmatrix} 2[N(1,i)]^4 (4 - 3M_i) + 3N(+,i) + N(\perp',i) + N(2,2,i) + \frac{1}{2} [N(2,i)]^2 (4 - M_i) \\ +4[N(1,i)]^2 (N(2,i)M_i + 3N(1,1,i)) - 4N(1,i)(N(3,i) + N(1,2,i) + 3N(\perp,i)) \\ +N(3,i) + 2N(\perp,i) - 8N(1,i)N(2,i) + 8[N(1,i)]^3 + 2z[N(1,i)]^2 - zN(2,i) \end{pmatrix}$$
(45)
$$\mathcal{Q}_{0,i}^{(s)} = \frac{1}{z^2} \begin{pmatrix} 3N(+,i) + N(\perp',i) + N(2,2,i) - \frac{1}{2} [N(2,i)]^2 M_i + 2N(\perp,i) + 2[N(1,i)]^4 \\ +4N(1,1,i)[N(1,i)]^2 - 2[N(1,i)]^4 M_i + 2[N(1,i)]^2 N(2,i)M_i \\ +[N(2,i)]^2 - 2N(1,i)N(3,i) - 6N(1,i)N(\perp,i) - 2N(1,i)N(1,2,i) \\ +\frac{8}{3} [N(1,i)]^3 - 4N(1,i)N(2,i) + N(3,i) + z[N(1,i)]^2 - zN(2,i) \end{pmatrix}$$
(46)

The first and second order energy contribution can also be developed in a polynomial of the void segment fractions [111,112]:

_

$$\frac{E_{1,0i,comp}}{N_l k_B T} = \frac{\mathcal{E}_{ii}}{k_B T} \sum_{p=0}^5 Q_{p,iv}^{(\varepsilon)} \phi_v^p \tag{47}$$

Here ε_{ii} is the interaction energy between two segments of component *i*. Again, the coefficients of the polynomial can be expressed in terms of the molecule's structure and the lattice coordination number [111,112]:

$$Q_{5,iv}^{(\varepsilon)} = -\frac{4}{z} \left[N(1,i) \right]^3$$
(48)

$$Q_{4,i\nu}^{(\varepsilon)} = -\frac{2}{z} \left(\left[N(1,i) \right]^3 \left(M_i - 6 \right) - 2N(1,i)N(1,1,i) - 2\left[N(1,i) \right]^2 \right)$$
(49)

$$Q_{3,i\nu}^{(\varepsilon)} = -\frac{1}{z} \begin{pmatrix} -4[N(1,i)]^3 M_i + 8N(1,i)N(1,1,i) + 8[N(1,i)]^2 - 3N(\perp,i) - N(1,2,i) \\ -N(3,i) + N(1,i)N(2,i)M_i - 2N(2,i) + zN(1,i) + 12[N(1,i)]^3 \end{pmatrix}$$
(50)

$$Q_{2,iv}^{(\varepsilon)} = \frac{1}{z} \begin{pmatrix} -N(1,2,i) + N(1,i)N(2,i)M_i - 3N(\perp,i) - N(3,i) - 2N(2,i) + zN(1,i) \\ +\frac{z^2}{2} + 4\left[N(1,i)\right]^3 - 2\left[N(1,i)\right]^3 M_i + 4N(1,i)N(1,1,i) + 4\left[N(1,i)\right]^2 \end{pmatrix}$$
(51)

$$Q_1^{(\varepsilon)} = -z \tag{52}$$

$$Q_0^{(\varepsilon)} = \frac{z}{2} \tag{53}$$

The same procedure for the second order energy contribution leads to [111,112]:

$$-\frac{E_{2,0i,comp}}{N_l k_B T} = \left(\frac{\boldsymbol{\varepsilon}_{ii}}{k_B T}\right)^2 \sum_{p=2}^6 Q_{p,iv}^{(\varepsilon^2)} \phi_v^p \tag{54}$$

where the polynomial coefficients can be calculated as [111,112]:

$$Q_{6,iv}^{(\varepsilon^2)} = 3 [N(1,i)]^2$$
(55)

$$Q_{5,i\nu}^{(\varepsilon^2)} = -8[N(1,i)]^2 + \frac{1}{2}[N(1,i)]^2 M_i - N(1,1,i) - 2N(1,i)$$
(56)

$$Q_{4,i\nu}^{(\varepsilon^2)} = 7 [N(1,i)]^2 - \frac{1}{2} [N(1,i)]^2 M_i + N(1,1,i) + 4N(1,i) - N(2,i) + \frac{z}{4}$$
(57)

$$Q_{3,iv}^{(\varepsilon^2)} = -2\left[N(1,i)\right]^2 - \frac{5}{2}N(1,i) + N(2,i) - \frac{z}{2}$$
(58)

$$Q_{2,i\nu}^{(\varepsilon^2)} = \frac{1}{2}N(1,i) + \frac{z}{4}$$
(59)

Helmholtz free energy can now be expressed as [111,112]:

$$-\frac{F_{comp}^{LCT}}{N_{l}k_{B}T} = \frac{S_{0i,comp}}{N_{l}k_{B}} - \frac{E_{1,0i,comp}}{N_{l}k_{B}T} - \frac{E_{2,0i,comp}}{N_{l}k_{B}T}$$
$$= -\phi_{v} \ln \phi_{v} - \frac{(1-\phi_{v})}{M_{i}} \left(\ln (1-\phi_{v}) + \ln \frac{2z}{M_{i}} - M_{i} \ln z + M_{i} - 1 \right)$$
$$+ \sum_{p=0}^{4} Q_{p,i}^{(s)} \phi_{v}^{p} + \frac{\varepsilon_{ii}}{k_{B}T} \sum_{p=0}^{5} Q_{p,iv}^{(\varepsilon)} \phi_{v}^{p} + \left(\frac{\varepsilon_{ii}}{k_{B}T}\right)^{2} \sum_{p=2}^{6} Q_{p,iv}^{(\varepsilon^{2})} \phi_{v}^{p}$$
(60)

From the Helmholtz free energy the thermal equation of state (LCT-EOS) can be calculated via standard thermodynamic relationships (Equation (4)) [111,112]:

88

$$P = -\left(\frac{\partial F_{comp}^{LCT}}{\partial V}\right)_{T,N_{i}} = -\frac{1}{\sigma_{i}^{3}} \left(\frac{\partial F_{comp}^{LCT}}{\partial N_{v}}\right)_{T,N_{i}}$$

$$= \frac{k_{B}T}{\sigma_{i}^{3}} \left[-\ln(\phi_{v}) - (1-\phi_{v})\left(1+\frac{1}{M_{i}}\right) + Q_{p,0}^{(s)} + \sum_{p=1}^{4} \left(p - (p-1)\phi_{v}\right)Q_{p,i}^{(s)}\phi_{v}^{p-1}\right) + \frac{\varepsilon_{ii}}{k_{B}T} \left(Q_{p,iv}^{(\varepsilon)} + \sum_{p=1}^{5} \left(p - (p-1)\phi_{v}\right)Q_{p,iv}^{(\varepsilon)}\phi_{v}^{p-1}\right) + \left(\frac{\varepsilon_{ii}}{k_{B}T}\right)^{2} \sum_{p=2}^{6} \left(p - (p-1)\phi_{v}\right)Q_{p,iv}^{(\varepsilon^{2})}\phi_{v}^{p-1}$$
(61)

Here, σ_i is the length of a cubic cell, a segment of molecule *i* occupies. The specific volume of the substance can be calculated with the following equation:

$$v = \frac{M\sigma_i^3}{1 - \phi_v} \tag{62}$$

The chemical potential of the species is given by [111,112]:

$$-\frac{\mu_{0i}}{k_{B}T} = -\frac{1}{k_{B}T} \left(\frac{\partial F_{comp}^{LCT}}{\partial N_{i}}\right)_{T,N_{v}}$$

$$= -\ln\left(1-\phi_{v}\right) - \ln\frac{2z}{M_{i}} + M_{i}\ln z - M_{i} + 1 + \phi_{v}\left(M_{i}-1\right) - M_{i}\sum_{p=1}^{4} (p-1)Q_{p,i}^{(s)}\phi_{v}^{p} \qquad (63)$$

$$-M_{i}\frac{\varepsilon_{ii}}{k_{B}T}\sum_{p=1}^{5} (p-1)Q_{p,iv}^{(\varepsilon)}\phi_{v}^{p} - M_{i}\left(\frac{\varepsilon_{ii}}{k_{B}T}\right)^{2}\sum_{p=2}^{6} (p-1)Q_{p,iv}^{(\varepsilon^{2})}\phi_{v}^{p}$$

Constant parts do not play a role in equilibrium calculations, as they are equal for both phases. This results in a simpler form for the chemical potential [111,112]:

$$\frac{\mu_{0i}^{eq}}{M_i k_B T} = \frac{1}{M_i} \ln\left(1 - \phi_v\right) - \phi_v \left(1 - \frac{1}{M_i}\right) + \sum_{p=1}^4 (p-1) Q_{p,i}^{(s)} \phi_v^p + \frac{\varepsilon_{ii}}{k_B T} \sum_{p=1}^5 (p-1) Q_{p,iv}^{(\varepsilon)} \phi_v^p + \left(\frac{\varepsilon_{ii}}{k_B T}\right)^2 \sum_{p=2}^6 (p-1) Q_{p,iv}^{(\varepsilon^2)} \phi_v^p$$
(64)

Differences to Section 2.2.1 occur, because of the reversed indexing of the solvent (or in this case the void lattice sites) and the not-specified other compound.

The multi-component expressions are somewhat more extended. Recently [111,112], the first formulation of the multi-component LCT only in terms of $\Delta \varepsilon_{ij} = \varepsilon_{ii} + \varepsilon_{jj} - 2\varepsilon_{ij}$ was developed. The interaction energy difference between a segment and a void lattice site becomes $\Delta \varepsilon_{iv} = \varepsilon_{ii}$, because of the vanishing energies ε_{iv} and ε_{vv} . Using the same strategy discussed above leads to power series allowing the calculation of the Helmholtz energy and all other thermodynamic properties [111,112]. The formulation in terms of $\Delta \varepsilon_{ij}$ and the reformulation of the Helmholtz free energy reduces the number of terms necessary to calculate from 103 [89–91] to 21 [111,112]. All coefficients depend only on the species' chemical architecture and the lattice coordination number. The component indices range from zero to the number of components present in the mixture k, where zero is the index of voids.

2.2.3. Application to Hyperbranched Polymers

Modelling phase behaviour of polymers by the LCT requires the estimation of the architectural parameters. These parameters can be determined only by the knowledge of the chemical structure of the polymer.

The number of monomers M can be evaluated by counting the repeating unit of a polymer chain. Also the number of bonds N_1 is independent of the polymers' branching architecture and can be calculated as follows [113]:

$$N_1 = M - 1$$
 (65)

All other topological coefficients of Table 1 depend on the architecture of the polymer. This architecture is described by the number of branching points b_i , where *i* describes the branching degree, that means the number of bonds which meet at one repeating unit.

М	Number of repeating units in a polymer chain
N_1	Number of bonds in a polymer chain
N_2	Number of two consecutive bonds in a polymer chain
N_3	Number of three consecutive bonds in a polymer chain
N_4	Number of four consecutive bonds in a polymer chain
$N_{1,1}$	Number of distinct ways of selecting two non-sequential bonds on the same chain
N _{1,2}	Number of distinct ways of selecting two sequential bonds and one non-sequential bond on the same chain
N _{2,2}	Number of distinct ways of selecting two non-sequential double consecutive bonds on the same chain
N_{\perp}	Number of ways in which three bonds meet at a lattice site for a polymer chain
N_+	Number of ways in which four bonds meet at a lattice site for a polymer chain
$N_{\perp'}$	Number of ways in which three bonds meet at a lattice site for a polymer chain and one bond is at this lattice site

Table 1. Topological coefficients of the LCT for an arbitrary polymer chain.

The total number of branching points is [113]:

$$b_{+} = \sum_{i=3}^{z} b_{i} \tag{66}$$

where b_i is the number of branching points of degree *i* in which *i* bonds meet.

As an example the determination of the coefficient N_2 will be shown. For a linear polymer in Figure 3 (first row) with three bonds, there are two possibilities of choosing two consecutive bonds in a linear polymer with three bonds. The chosen bonds are marked by broken lines. This can be generalized for a linear polymer with M monomers as follows [113]:

$$N_{2,l} = M - 2 \tag{67}$$

where $N_{2,l}$ denotes N_2 for a linear chain.

If there is one point with branching degree of three, the number of ways of choosing two consecutive bonds is raised by one per branching point in contrast to linear chains (Figure 3, second row). By appearing of a branching point of branching degree of 4, there are three more possibilities in

comparison to a linear chain (Figure 3, third row). This can be generalized to higher branching degrees as can be seen in Table 2; whereas it has to be mentioned that in polymer chains only branching points with degree up to four exists. With help of Table 2 an equation can be derived, which can be used to calculate the number of possibilities [113]:

$$N_2 = N_{2,l} + \sum_{i=3}^{z} \frac{(i-1)(i-2)}{2} b_i$$
(68)

Figure 3. Number of two consecutive bonds up to a branching degree of four.

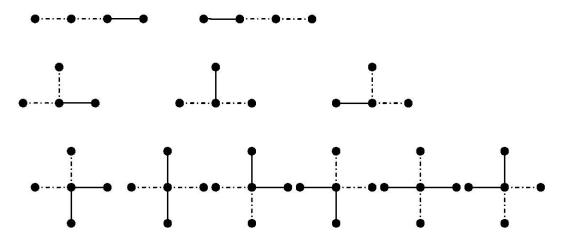


Table 2. Number of additional possibilities of choosing two consecutive bonds on a polymer chain with branching degree up to seven.

Additional possibilities of		
Branching degree	choosing two consecutive bonds	
3	1	
4	3	
5	6	
6	10	
7	15	

The factor i is reduced by each chosen bond and the factor 1/2 appears because of the indistinguishability. In an analogous manner the number of ways of choosing three or four bonds can be described [113]:

$$N_3 = N_{3,l} + \sum_{i=3}^{z} (i-1)(i-2)b_i$$
(69)

$$N_4 = N_{4,l} + \sum_{i=3}^{z} \frac{3(i-1)(i-2)}{2} b_i$$
(70)

where $N_{i,l}$ describes the contribution of a linear chain [113]:

$$N_{i,l} = M - i \tag{71}$$

Equation (69) requires that there are at least two bonds between two branching points and Equation (70) implies that there are at least three bonds between two branching points. Another class of coefficients are the number of n bonds meeting at one lattice site. As an example the number of three bonds N_{\perp} meeting at one lattice site is derived.

Figure 4 shows different ways of choosing three bonds meeting at one lattice site (monomer). The different ways are shown by broken lines. If there is a point with branching degree of three, there is only one way of choosing three bonds at one lattice site, but for a point of branching degree of four there are four ways. This can be generalized to higher branching degrees as shown in Table 3.

Figure 4. Number of ways of three bonds meeting at one lattice site up to a branching degree of four.

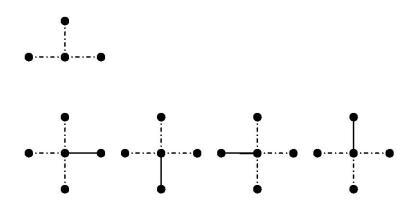


Table 3. Number of ways of choosing three bonds meeting at one lattice site up to branching degree of seven.

Ways of choosing three bonds		
Branching degree	at one lattice site	
3	1	
4	4	
5	10	
6	20	
7	35	

With help of Table 3 or combinatorial considerations the following equation can be derived [113]:

$$N_{\perp} = \sum_{i=3}^{z} \frac{i(i-1)(i-2)}{6} b_i$$
(72)

Here, the factor *i* is the number of points meeting at one lattice site which is reduced by one for each chosen bond and the factor 6 appears because of the indistinguishability. In a similar way the coefficient N_{+} can be determined [113]:

$$N_{+} = \sum_{i=3}^{z} \frac{i(i-1)(i-2)(i-3)}{24} b_{i}$$
(73)

The number of ways three bonds meeting at one lattice site with one additional bond can then calculated by:

$$N_{\perp'} = 3N_{\perp} \tag{74}$$

The last group of architectural coefficients to be determined are the bonds lying on the same chain but are not sequential. As an example the determination of the coefficient $N_{1,1}$ will be shown [113]:

$$N_{1,1} = \frac{N_1^2 - N_1 - 2N_2}{2} \tag{75}$$

On the right hand side the first term describes the number of selecting two bonds on a chain without restriction, whereas the second term excludes the counting of the same bond twice and the third excludes the sequential bonds. The factor 1/2 arises because of the indistinguishability of the chosen ways.

In the same way, the factors $N_{2,1}$ and the factor $N_{2,2}$ can be determined [113]:

$$N_{2,1} = N_1 N_2 - 2N_2 - 2N_3 - 3N_\perp$$
(76)

$$N_{2,2} = \frac{N_2^2 - N_2 - 2N_3 - 2N_4 - 6N_\perp - 2N'_\perp - 6N_+}{2}$$
(77)

The architecture of the polymer can be described with help of the number of segments and the number of branching points with degree, n. With help of the presented parameters, the K_i and the L_i that occur in the incompressible version and N(i, j) for the compressible version can be calculated as follows:

$$K_{1} = N_{1;1} / M_{1}; \quad K_{2} = N_{2;1} / M_{1}; \quad K_{3} = N_{3;1} / M_{1};$$

$$K_{4} = N_{\perp;1} / M_{1}; \quad K_{5} = N_{1,1;1} / M_{1}; \quad K_{6} = N_{1,2;1} / M_{1};$$
(78)

$$L_{1} = N_{1,2} / M_{2}; \quad L_{2} = N_{2,2} / M_{2}; \quad L_{3} = N_{3,2} / M_{2}; \quad (79)$$

$$L_{4} = N_{\perp;2} / M_{2}; \quad L_{5} = N_{1,1;2} / M_{2}; \quad L_{6} = N_{1,2;2} / M_{2}$$

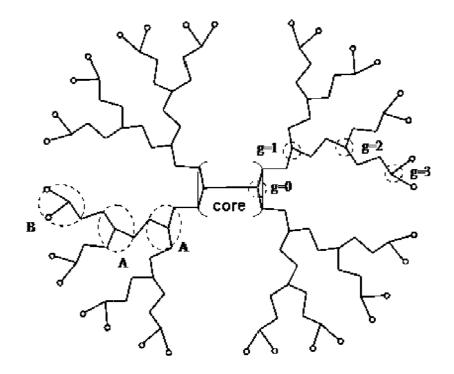
$$N(1,i) = N_{1,i} / M_{i}; \quad N(2,i) = N_{2,i} / M_{i}; \quad N(3,i) = N_{3,i} / M_{i}$$

$$N(\perp,i) = N_{\perp,i} / M_{i}; \quad N(\perp',i) = N_{\perp',i} / M_{i}; \quad N(+,i) = N_{1,i} / M_{i}$$

$$N(1,1,i) = N_{1,1;i} / M_{i}; \quad N(1,2,i) = N_{1,2;i} / M_{i}; \quad N(2,2,i) = N_{2,2;i} / M_{i}$$
(80)

where the number as additionally subscript of the architectural parameters indicates the component number.

Figure 5. Schematic sketch of a hyperbranched polymer of generation number g = 3 [93].



As an example for determining the architectural parameters, three different hyperbranched polyesters with the generation numbers g = 2 (Boltorn H20), g = 3 (Boltorn H30) and g = 4 (Boltorn H40) will be regarded [53]. All these molecules possess the same core: $O[CH_2C(C_2H_5)(CH_2O-)_2]_2$. Depending on the generation number g, the molecules additionally include a different number of groups A: $COC(CH_3)(CH_2OH-)_2$. and B: $COC(CH_3)(CH_2OH)_2$. The general formulae of the polymers are for g = 2: $(core)A_4B_8$, for g = 3: $(core)A_{12}B_{16}$ and for g = 4: $(core)A_{28}B_{32}$. According to these formulae (neglecting polydispersity) the molar masses take the values 1,642 g/mol (g = 2), 3,498 g/mol (g = 3) and 7,210 g/mol (g = 4). The number of OH– end groups equals the number of B-units. Figure 5 shows schematically a hyperbranched polyester with the generation number g = 3.

To describe the architecture of a hyperbranched polymer two specifications in addition to the generation number g will be used [53]. The separator length n is the number of segments between two branching points. It denotes the number of segments of an A unit or a B unit. The number of core segments is given by the quantity, n_0 . It is assumed that one water molecule occupies one lattice site, so the number of core segments and the separator length can be determined by dividing the core, A and B units in groups that have a molar mass comparable to a water molecule. The values of the separator length, number of core segments and generation number are collected in Table 4.

Separator length <i>n</i>	4
Number of core segments n_0	7
Generation number g	g = 2 (Boltorn H20)
	g = 3 (Boltorn H30)
	g = 4 (Boltorn H40)

Table 4. Architectural parameters describing hyperbranched polyester [53].

Using these architectural parameters, the topological coefficients of the LCT can be calculated. The number of segments of a hyperbranched polyester molecule can be calculated as follows [53]:

$$M = 4(2^{g} - 1)n + n_{0}$$
(81)

Each A-unit and each B-unit possesses one branching point of degree 3. The core contains two such branching points. Branching points of degree 4 and higher do not exist in these polymer molecules and hence the number of branching points is calculated as follows:

$$b_3 = 4(2^g - 1) + 2 \tag{82}$$

Using these parameters the LCT can be applied to polymer solutions containing one of the presented polymers.

Another polymer, which is considered, is Boltorn U 3000 [57]. This HBP has the molar mass 7,192 g/mol. The molecule consists of the core $C(CH_2O-)_4$, 12 separator groups *A*: $COC(CH_3)(CH_2OH-)_2$. and 16 groups *B*: $COC(CH_3)(CH_2OH)(CH_2OR)$ with the end groups *OH* and *OR*. Here, *R* origins from the 16-carbon-long alkyl acid (*R*: $CH_3-(CH_2)_{14}CO-$). The core is divided into 5 segments and the separator group A into 4 segments. Considering the 16-carbon-long group *R* the group *B* has 20 segments. All together a Boltorn U3000 molecule may be described by $M_B = 373$ segments. Furthermore, there are 28 branching points of degree 3 ($b_3 = 28$) and one branching point of degree 4 ($b_4 = 1$).

2.3. Wertheim Theory

The hyperbranched polymers of the Boltorn family carry hydroxyl groups able to form hydrogen bonds, not only associates between two polymer molecules and between other polar groups of the same polymer molecule but also with solvents present in the solution. Žagar and Grdadolnik [114] and Žagar and Žigon [52] used IR-spectroscopy to analyze the extent and the type of hydrogen-bonds. They [52,114] pointed out that the majority of the hydroxyl groups are hydrogen-bonded in four diverse assemblies, differing in strength. The effect of intermolecular and intramolecular interaction caused by the polar groups were investigated experimentally by Turky *et al.* [115] using dielectric spectroscopy and theoretically by Tanis and Karatasos [116] by atomistic molecular dynamics simulation. Both studies [115,116] concluded that the intramolecular interactions are stronger than the intermolecular interactions. For this reason intramolecular as well as intermolecular association should be taken into account in the thermodynamic model.

A model for a fluid with directional attractive forces is a fluid of hard particles with an off-center spot that is the origin of an attractive potential. The formation of an attractive interaction needs the orientation of two particles towards each other in such a way that the attractive potentials are within each other's reach. In the case of a short ranged attractive potential originated near the edge of a spherical particle, so that there can only one bond per particle, the directional attraction has the character of a bond between two particles.

The formalism used here was developed by Wertheim [73–76]. Wertheim has established a general statistical mechanical framework for fluids of particles that exhibit directional forces and attractions. His work originally focused on particles that have one off-center attractive spot [73,74] and was later generalized to include more off-center spots per particle [75,76]. The method, the multiple density formalism, which reduces to a 2-density formalism for singly associating fluids, is based on a separation of the interparticle potential in a purely repulsive isotropic part and an attractive potential that is a function of the particle orientation. This separation allows dividing the overall particle density in a density of non-bonded particles, and in a density of particles that have formed a bond with another particle.

2.3.1. Derivation of the Association Theory

In Wertheim's approach [73–76], the overall density of particles in the fluid is divided in two parts. For a fluid consisting of particles with one attractive spot the formalism is in terms of two densities: the overall particle density ρ is divided into a density of non-bonded particles ρ_0 and a density of particles ρ_1 forming an attractive bond with another particle [73]:

$$\rho = \rho_0 + \rho_1 \tag{83}$$

In a fluid of particles with only one attractive spot, bonded and non-bonded particles are present. The total 2-particle distribution function G(1,2) is constituted from contributions arising from the correlations between two particles which have not formed an attraction bond $g_{00}(1,2)$, two particles of which one has formed an attraction bond $g_{10}(1,2)$ and $g_{01}(1,2)$, and two particles that both have formed an attraction bond $g_{11}(1,2)$. The coordinates of particles 1 and 2 are given by (r_1, Ω_1) and (r_2, Ω_2) , where r_i denotes the position and Ω_i the orientation of particle *i*.

To get a multiple density approach, the pair interaction potential u(1,2) depending on the orientation of particle 1 and 2 can be split in two parts, an isotropic repulsive part $u_R(r_1,r_2)$ and a directional attractive part $u_{att}(1,2)$. The Mayer function f(1,2) can be divided in an attractive F(1,2) and a purely repulsive part $f(r_1,r_2)$ [73]:

$$f(1,2) = f_R(r_1, r_2) + F(1,2)$$
(84)

with

$$f_{R}(r_{1}, r_{2}) = \exp\left(\frac{-u_{R}(r_{1}, r_{2})}{k_{B}T}\right) - 1$$
(85)

and

$$F(1,2) = \exp\left(-\frac{u_R(r_1,r_2)}{k_BT}\right) \left(\exp\left(-\frac{u_{att}(1,2)}{k_BT}\right) - 1\right)$$
(86)

It has been proven [73,74] that this division of the Mayer function allows a diagrammatic expansion of ρ in terms of the activity z, f_R - and F-bonds similar to LCT. According to the suggested expansion, the overall density ρ is devided into densities of bonded and non-bonded particles. The ρ_0 and ρ_1 -values are then both classified by a different part of the set of diagrams that constitutes ρ . Starting from the grand canonical partition function $\Xi(\mu, V, T)$ and applying these expansions of ρ_0 and ρ_1 , Wertheim [73,74] derived an exact diagrammatic expansion of the structural correlations $g_{00}(1,2)$, $g_{01}(1,2)$, $g_{10}(1,2)$ and $g_{11}(1,2)$ in terms of ρ_0 and ρ_1 , f_{R} - and F-bonds. He then constituted, along the same lines as the direct correlation function is defined, for fluids consisting of hard spheres, partial direct correlation functions $c_{00}(1,2)$, $c_{01}(1,2) = c_{10}(1,2)$ and $c_{11}(1,2)$ and received their diagrammatical expansions in terms of ρ_0 , ρ_1 and $f_R(1,2)$ and F(1,2). The partial correlation is related to the Orstein-Zernicke equations. This procedure bears strongly resemblance to the derivation of the Orstein-Zernicke equation for hard spheres [117-119]. To obtain the fluid structure, the Orstein-Zernicke matrix equation has to be combined with an appropriate radial distribution function $g(r_1, r_2)$ as a closure equation and a self consistency relation based on Equation (83). The self consistency relation is a mass balance equation determining the division in bonded and non-bonded particles. For fluids without directional forces the Orstein–Zernicke equations and a closure equation determine the fluid structure in terms of particle density ρ . For a fluid with directional forces, the Orstein-Zernicke equations and a closure equation generate the correlations $g_{00}(1,2), g_{10}(1,2)$ and $g_{11}(1,2)$ in terms of ρ_0 and ρ_1 .

These correlations define the distribution of the particles over bonded and non-bonded particles. For fluids consisting of hard spheres this distribution is not possible, because there is only one type of particles left. For fluids with directional attractive forces, the ρ_0 and ρ_1 functions assign $g_{00}(1,2)$, $g_{10}(1,2)$ and $g_{11}(1,2)$ with help of Orstein–Zernicke equations and on the other hand the $g_{00}(1,2)$, $g_{10}(1,2)$ and $g_{11}(1,2)$ determine the values of ρ_0 and ρ_1 . This last step is necessary for internal consistency and is provided by the self-consistency relation. The Wertheim theory has three constituent parts, the Orstein–Zernicke equations, a closure equation and a self-consistence mass balance equation. Wertheim extended this formalism to a multi-component mixture with different interaction sites [75,76]. In the following section the use of Wertheim association theory for a polymer blend will be shown.

2.3.2. Wertheim Association Theory for a Polymer Blend

As the LCT has no information about the density of the polymer blend, another version of the Wertheim theory than used in the SAFT equations of state [72,77] has to be used. The presented version of the Wertheim theory is a Lattice Wertheim theory suggested by Nies *et al.* [120,121]. The Wertheim theory was transferred to a fully occupied lattice, so an incompressible fluid is regarded. The following expression for the Helmholtz energy of association was derived [73–76]:

$$\frac{f_{asso}}{k_B T} = \sum_{i} \Phi_i \left[\sum_{A_i} \left[\ln \left(X_{A_i} \right) - \frac{X_{A_i}}{2} \right] + \frac{1}{2} M_i^{Asso} \right]$$
(87)

where X_{Ai} is the segment molar fraction of the non-bonded polymer segments and M_i^{Asso} is the number of association sites at one molecule. "Non-bonded polymer segments" means in this case that the segments do not contribute to association. The value X_{Ai} is given by:

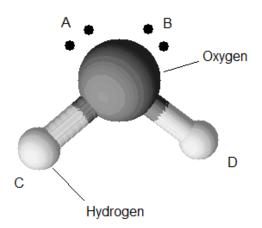
$$X_{A_i} = \left[1 + \sum_j \sum_{B_j} \Phi_j X_{A_j} \Delta^{A_i B_j}\right]^{-1}$$
(88)

where the summation over B_j runs over all molecules and association sites. The association strength, $\Delta^{A_i B_j}$, is given by:

$$\Delta^{A_i B_j} = K_i^{Asso} \left(\exp\left(\frac{\varepsilon_{ij}^{Asso}}{k_B T}\right) - 1 \right)$$
(89)

with K_i^{Asso} being the ratio of nearest-neighbour positions with the proper orientation to all possible orientations of the component *i* and \mathcal{E}_{ij}^{Asso} is the association energy. The difference between the Lattice Wertheim association model and the association model used in the SAFT equation of state lies in the considerations of the quantity K_i^{Asso} occurring in Equation (89) and the similar quantity, κ , called association volume. The association volume κ depends on the density and the radial distribution function. In contrast, K_i^{Asso} is a constant. For example a water molecule has four association sites, one at each proton of the hydrogen and one at each lone electron pair of the oxygen (Figure 6).





After the localization of the association sites, the possible interactions of the association sites have to be defined; for instance that only a proton and a lone electron pair can interact with each other and not two proton sites or two electron pair sites. This leads, for multi-component cross associating systems, to a nonlinear equation system of equations of type Equation (88), which has to be solved numerically to calculate the Helmholtz free energy. Recently [122], a notation was developed in order to solve this non linear equation system of equations in an elegant way. In opposite to this, in the case of only one associating molecule, the association can be determined analytically. To consider the association between different molecules mixing rules for the association volume and the association energy are applied to calculate the parameters for the cross-association:

$$K_{ij}^{Asso} = \frac{K_i^{Asso} + K_j^{Asso}}{2}$$
(90)

and

$$\varepsilon_{ij} = (1 - k_{ij})\sqrt{\varepsilon_{ii}\varepsilon_{jj}}$$
(91)

The parameter k_{ij} was introduced to consider the deviation of the interaction energy from the geometrical mixing rule [58,123].

3. Calculation Examples

The presented theoretical framework can be applied to investigate the miscibility of polymer solutions and polymer mixtures.

3.1. Binary Polymer Solutions

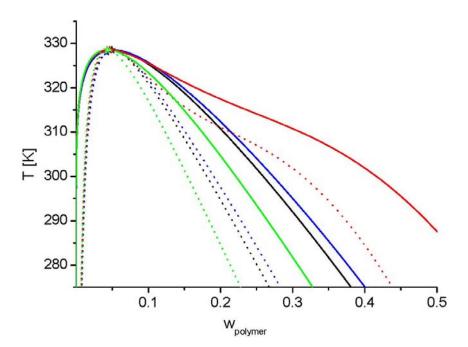
Within a certain polymer concentration range, a polymer-poor solvent solution phase separates into a polymer-lean and a polymer-rich phase to minimize its overall free energy depending on the enthalpic interactions and the mixing entropy. Like mentioned in Section 2, the LCT is a further extension of the well-known FH theory. In order to study the achieved improvements, some model calculations for linear polymers with a segment number of $M_1 = 500$ dissolved in solvent occupying only one lattice site $(M_2 = 1)$ were performed. Using the FH theory for this purpose mostly leads to a prediction of a too narrow miscibility gap. This problem can be solved, if the χ parameter in Equation (17) is expressed phenomenological as a power series of the polymer concentration. Figure 7 depicts a comparison of the modelled phase equilibrium using the FH theory and the LCT. The interaction parameter ($\Delta \varepsilon / k_B$ or χ) were fitted to an arbitrarily selected critical temperature. In the FH-limit the lattice coordination number z approaches infinity. In the LCT framework z can be chosen. On one side z should be large in order to ensure a rapid convergence of the suggested series in 1/z. On the other hand a lower number for z makes more use of the established corrections. For this reason some model calculations for different z-values were performed. In Figure 7 it can be seen that a higher z-value requires a lower interaction energy for the same critical temperature. The miscibility gap gets broader, independently of the chosen z-value of the LCT. Sometimes a shoulder in the cloud point curve [83] is found experimentally. Examples are the systems polystyrene + cyclohexane and polyethylene + diphenylether [83]. This effect is often explained by polydispersity or by a complex concentration dependence of the χ -parameter. The calculation results for z = 6 in Figure 7 show this

shoulder for a monodisperse linear polymer. Therefore, the shoulder could also be discussed in terms of mixing entropy. In summary, the LCT can also be used for linear polymers, especially if complex phase diagrams are present. It is well-known that the classic Flory–Huggins theory [84,85] does not capture the effect of branching on polymer phase separation. The polymer theories which do capture the effect of branching include a scaling theory developed by Daoud *et al.* [65] a theory developed by Saeki [124], which replaces the standard mixing entropy term of Flory–Huggins with a combinatorial

entropy term more applicable to star polymers, and the lattice cluster theory due to Freed and co-workers (e.g., [89]). All these theories predict a drop in the critical temperature and a small rise in the critical polymer concentration as a polymer becomes more branched. However, the lattice cluster theory is the most sophisticated of the three theories mentioned above.

The mixing entropy and enthalpy are complex functions of the polymer structure. Intuitively, one expects that a branched polymer will display fewer unfavorable polymer-solvent interactions than a linear polymer with an identical molecular weight [125]. This would imply that the branched polymers should exhibit an increased miscibility and lower upper critical solution temperatures as compared to linear polymers. Alessi *et al.* [126] observed that the critical temperatures of branched (star-shaped with 8 arms) polystyrene (PS) in methyl cyclohexane (MCH) solvent were 5–15 K lower than that for linear polystyrene of the same molecular weight in the same solvent, and the difference decreased as the molecular weight of the polymer increased. From the viewpoint that branched polymers are generally more compact than their linear counterparts, we expect that the critical volume fraction of branched polymers should exceed that of the linear polymers with similar molecular weights.

Figure 7. Calculations of LLE for the system linear polymer $(M_1 = 500)$ in a solvent occupying only one lattice site $(M_2 = 1)$ (solid line: binodal line, dotted line: spinodal line, stars: critical points), where the black colour depicts the results using the LCT with z = 12; $\varepsilon/k_B = 35 \ K$, the blue colour those with z = 10; $\varepsilon/k_B = 43.86 \ K$, the red colour those with z = 6; $\varepsilon/k_B = 93.62 \ K$, and the green colour presents the results obtained by FH theory with $z \to \infty$; $\chi = 0.54572$.



Yokoyama *et al.* [127] observed that the critical volume fraction was equal to 0.03 and 0.04 for linear and 6.3-arm PS in cyclohexane solvent, respectively. This means that the more compact branched polymers need to be present at higher concentrations than their more extended linear counterparts in order to interact at the same degree with each other as the linear polymers do. Hence, branched polymers begin to phase separate at higher polymer concentrations than the polymer concentrations required by linear polymers to phase separate. However, Alessi *et al.* [126] on the other hand, do not show any noticeable differences in the critical volume fraction of star-shaped and linear versions of polystyrene in methyl cyclohexane solvent.

We will focus our attention to commercial available hyperbranched polymers from the Boltorn-family. Tables 5 and 6 list the model parameters. For the following calculations z was set to 12. Details about the fitting procedure and the used data are given in the literature [54–58].

Component	K_i^{Asso}	$\varepsilon_i^{Asso}/k_B[K]$	Ref.
Boltorn H20a ¹	0.023	1,200	[54]
Boltorn H20b ¹	0.023	1,200	[58]
Boltorn U3000	0.023	1,200	[55]
Water	0.01	1,800	[54]
Propan-1-ol	0.011	1,745	[56]
Butan-1-ol	0.01	1,710	[58]

Table 5. Pure-component parameters for the Lattice Wertheim Theory.

¹ These polymers have different lot numbers [58].

Component i	Component j	$\Delta \varepsilon_{ij}^{LCT}/k_B \ [K]^1$	$\Delta \varepsilon_{ij}^{LCT}/k_B [K]^{22}$	k _{ij}	Ref.
Boltorn H20a	Water	46.842	11.65	0.06	[58]
Boltorn H20b	Water	45.27	18.05	0.02	[58]
Boltorn H20a	Propan-1-ol	18.96	10.55	0.04	
Boltorn H20b	Butan-10l	14.983	9.01	0.035	[58]
Boltorn U3000	Propan-1-ol	12.59	3.9	0.03	
Boltorn U3000	Butan-1-ol	10.54	2.03	0.02	
Propan-1-ol	Water	64 (fitted to binary VLE)			[56]
		45 (fitted to ternary LLE)			
Butan-1-ol	Water	184.622	57.5	0.03	[58]

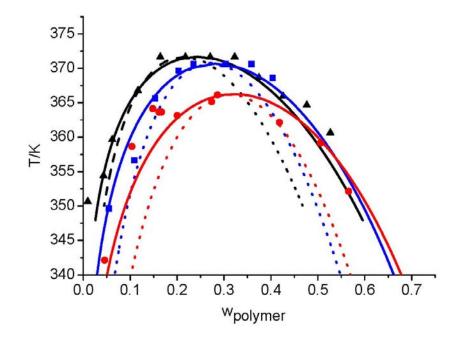
Table 6. Parameters of the mixture.

¹ These parameters are valid, if only the LCT is used; ² These parameters are valid, if the LCT in combination with the Wertheim theory is used.

The phase behaviour of Boltorn H20 in different polar solvents is shown in Figure 8, where the calculated LLE's are compared with experimental data [54,58]. The branch of the cloud-point curve for the diluted polymer solution in water and in propan-1-ol could be described in excellent agreement with experimental data, if the LCT either alone or in combination with the Wertheim theory is utilized (Figure 8). For the butan-1-ol containing solution some deviations occur, which can also be related to experimental difficulties [54]. Deviations between the experimental and theoretical cloud-point curve in the concentrated range occur for all studied polymer solutions, if only the LCT is applied. Taking

the association forces in terms of self- and cross association into account leads to an improvement of the calculated results by shifting the polymer mass fraction in the concentrated phases to larger values and hence the application of the Wertheim approach improves the calculation results in the right direction. Including only self-association and not cross association in the theoretical calculations leads to extremely high demixing temperatures [54], where the polymer is hardly stable. The calculation results agree with experimental findings only if both effects (self- and cross association) are taken into account (Figure 8).

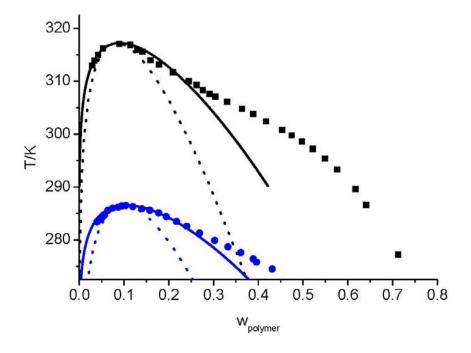
Figure 8. Phase behaviour of Boltorn H20 in different solvents (water: black triangles [54], propan-1-ol: blue squares [54], butan-1-ol: red circles [58]). The dotted lines are calculations based on LCT and the solid lines are calculations based on LCT + Wertheim approach, where the used parameters are listed in and Table 6 [54,58].



Similar to the results obtained for the system Boltorn H20 in polar solvents (Figure 8), the LCT in combination with the Wertheim approach describes the branch of the cloud point curve related to the diluted polymer solution very close to the experimental data for the system Boltorn U3000 in alcohol (Figure 9). However, for the branch of the cloud point curve describing the composition of the polymer-rich phase some deviations occur. For the system Boltorn U3000 + propan-1-ol the experimental cloud point curve shows a characteristic shoulder. Our theoretical framework was not able to describe this shoulder. One possible explanation for this situation can be the fixed z-value. Like shown in Figure 7 the LCT is in principle able to describe a shoulder in the cloud point curve.

The performance of the theory in describing the mixing behaviour in non-polar solvent, for instance *n*-alkanes, is discussed in the literature [57]. For the calculation of binary phase diagrams always one or more parameter must be adjusted to experimental data. The real strength of the theory can be recognized by investigation of the predictive power. This can be done if ternary mixtures are considered.

Figure 9. Phase behaviour of Boltorn U3000 in different solvents (propan-1-ol: black squares [128], butan-1-ol: blue circles [58]). The dotted lines are calculations based on LCT and the solid lines are calculations based on LCT + Wertheim approach, where the used parameters are listed in Tables 5 and 6 [55].

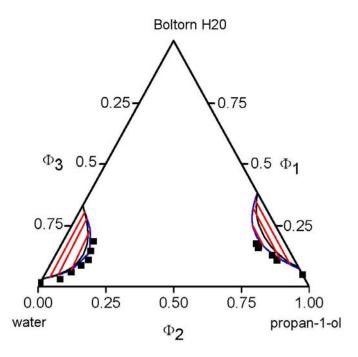


3.2. Ternary Polymer Solutions

The calculation of LLE of a ternary system using the LCT requires the knowledge of all three interaction parameters, $\Delta \varepsilon_{ii}$, of each component pair. For the analysis of the predictive power of the LCT, two mixtures were selected, namely Boltorn H20 + water + propan-1-ol and Boltorn H20 + water + butan-1-ol. Boltorn H20 + water as well as Boltorn + alcohol, either propan-1-ol or butan-1-ol, exhibit a LLE (Figure 8) and hence the interaction parameters for these subsystems can be estimated using the corresponding phase binary diagram [54,58]. The most important difference between these mixtures lies in the water-alcohol mixture, where water + butan-1-ol has a miscibility gap and water + propan-1-ol does not. For the ternary system Boltorn H20 + butan-1-ol + water, where all binary subsystems show a miscibility gap, all parameters can be estimated using LLE of the binary subsystems. In contrast, for the ternary Boltorn H20 + propan-1-ol + water the parameter describing the binary subsystem propan-1-ol + water must be adjusted to other thermodynamic properties. Experimentally, it was found that two separated miscibility gaps in the Gibbs triangle at constant temperature appear [56]. If the binary interaction parameter between the components of the mixed solvent is set to zero qualitative wrong phase behaviour with a miscibility gap ranged from the water-rich side to the propan-1-ol-rich side is predicted by the LCT [56]. One possibility to estimate this missing parameter is the use of VLE data for this system [56]. The VLE of the system water + propan-1-ol is characterized by an azeotropic point at atmospheric pressure. The interaction parameter was adjusted to the azeotropic temperature at atmospheric pressure, and at the same time the mole fraction at the azeotropic point is calculated exactly, because of the calculation of the activity coefficients with a high accuracy. Using this fitted parameter $\Delta \varepsilon_{23}/k_B = 64 K$ (Table 6) the experimental phase behaviour of the

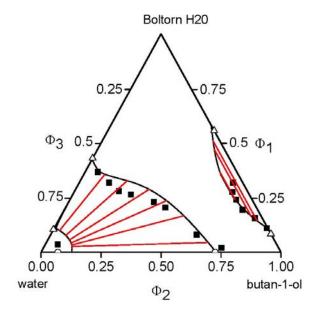
ternary system can be predicted quite close to the experimental data, like shown via the black lines in Figure 10. A slight readjustment of this parameter by changing its numerical value from $\Delta \varepsilon_{23}/k_B = 64 K$ to $\Delta \varepsilon_{23}/k_B = 45 K$ (Table 6) permits an excellent description of the ternary phase behaviour (blue lines in Figure 10).

Figure 10. Experimental (squares, [56]), predicted using LCT with the parameters in Table 6 (black lines, [56]), and fitted via changing the value for the binary interaction of water and propan-1-ol from 64 K to 45 K (blue line, [56]) ternary phase behaviour of Boltorn H20 + water + propan-1-ol at 353.15 K. The red lines are tie lines which are calculated with $\Delta \varepsilon_{12}^{LCT}/k_B = 45 K$.



For the other ternary system, built up from Boltorn H20 + water + butan-1-ol (Figure 11), all parameters are given from the binary subsystems (Tables 5 and 6), and hence the ternary phase behaviour can be predicted. The increased molecular weight of butan-1-ol in comparison with propan-1-ol leads to a qualitative different phase behaviour. For this system also two separated miscibility gaps at constant temperature appear. For both mixtures, the miscibility gap arising from the Boltorn H20 + alcohol side in the Gibbs triangle is very similar (Figures 10 and 11). The most important qualitative difference can be observed from the miscibility gap starting on the Boltorn H20 + water side. Caused by the occurrence of the water + alcohol demixing behaviour, this miscibility gap runs from the butan-1-ol containing system to the water + butan-1-ol side (Figure 11). This is in contrast to the propan-1-ol containing system, where the binary LLE of water + alcohol is missing (Figure 10). The interaction parameters were gained by fitting it to the phase behaviour of the binary subsystems. In Figure 11 it can be recognized that the LCT in combination with the Wertheim lattice approach is nicely able to predict the whole phase diagram at constant temperature in good agreement with the experimental data, also from the quantitative point of view. This situation verifies the predictive power of the applied theoretical framework and places emphasis on the role of hydrogen bonding in the system.

Figure 11. Experimental (solid squares, [58]; open circles [129], open triangles interpolation from the binary data [54,58]) and predicted (lines) ternary phase behaviour of Boltorn H20 + water + butan-1-ol at 353.15 K using LCT in combination with Wertheim lattice theory. The red lines are tie lines.



3.4. Polymer Mixtures

Recently [55], it was demonstrated that the LCT does a good job in modeling the experimental phase diagram of polymer mixtures, composed from linear polybutadiene and linear polystyrene with different molecular weights. Within the LCT we assumed every polystyrene monomer occupy one lattice site and every butadiene monomer two of them [55]. The question arising now is the miscibility of a hyperbranched polymer and a linear polymer. From the practical point of view, the miscibility of polymer blends is a critical issue, if a small amount of hyperbranched polymer is added to a linear polymer to reduce their melt viscosity. In this situation a miscibility gap is highly unwanted. Figure 12 demonstrates the cloud point curves occurring via adding the hyperbranched polymer Boltorn U3000 to a linear polymer having different segment numbers. It can be seen that a very small value of the interaction energy ($\Delta \varepsilon / k_B = 3 K$) creates a demixing, where the critical temperature depends strongly on the number of segments of the linear chain. For a short chain ($M_2 = 10$) the miscibility gap occurs at very low temperatures, which are not relevant in practical applications. A slight increase of the segment number from $M_2 = 10$ to $M_2 = 30$ shifts the demixing curve over 300 K to higher temperatures, where the polymers are hardly stable. This situation can be relevant in technical applications, because the demixing is undesirable. In all phase diagrams an upper critical solution temperature (UCST) occurs. If a homogeneous phase must be prepared, then the systems must be heated above the UCST. However, at this high temperature most polymers start to degrade. If the molecular mass of the linear counterpart increases further, then the critical point is above all realistic temperatures. Maybe, the cloud-point curve can be shifted to lower temperature by a small change of the enthalpic effects via incorporation of functional groups in the linear polymer. However, the dominant effect is the entropic penalty for these kinds of mixtures.

Figure 12. LCT model calculations of the mixing (symbols: critical point, lines: cloud point curves) behaviour of hyperbranched polymer Boltorn U3000 + linear polymers having different segment numbers (solid line: $M_2 = 10$, dashed line: $M_2 = 30$, dotted line: $M_2 = 50$), where $\Delta \varepsilon/k_B = 3 K$.

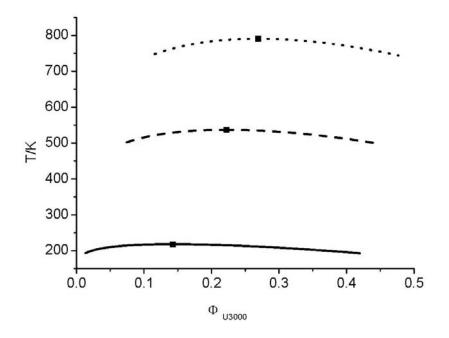


Figure 13. LCT model calculations of the mixing (symbols: critical point, lines: cloud point curves) behaviour of hyperbranched polymer Boltorn U3000 + hyperbranched polymer H20 (solid line), of Boltorn U3000 + H30 (dashed line) and Boltorn U3000 + H40 (dotted line), where $\Delta \varepsilon / k_B = 1 K$.

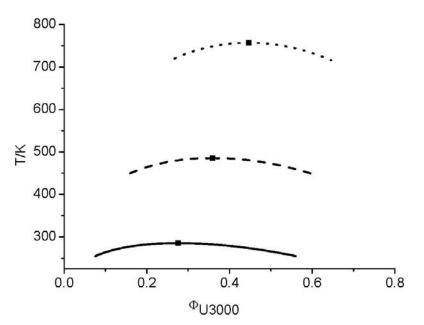
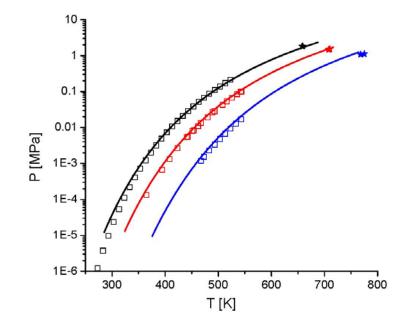


Figure 13 depicts the modelled phase behaviour if two different Boltorn hyperbranched polymers were mixed. If Boltorn H20 is mixed with Boltorn U3000 a miscibility gap with an UCST of 285 K occurs, even for a very small value for the interaction energy $\Delta \varepsilon / k_B = 1 K$. If Boltorn H30 is present the UCST and hence the demixing region shifts to much higher temperatures. This effect is caused by two

facts, first the molecular weight of Boltorn H30 is higher than the molecular weight of Boltorn H20 and second the generation number increases from g = 2 to g = 3. Increasing both characteristic features (the generation number g and consequently the segment number M_1) further leads to an UCST which is above the degradation temperature of the hyperbranched polymers. In other words, the LCT predicts that it is not possible to prepare a homogenous mixture made from Boltorn H40 and Boltorn U3000.

In this context it appears worth mentioning that blends of branched and linear polyisoprene exhibit a relatively broad miscibility gap at room temperature [130]. Samadi *et al.* [130] measured the ternary phase diagram of branched polyisoprene + cyclohexane + acetone at room temperature and compare this diagram with the phase diagram of linear polyisoprene + cyclohexane + acetone at the same temperature. In the phase diagram with the branched polyisoprene an uncommon peninsula of immiscibility protrudes from the normal two-phase area resulting from the binary subsystem polymer + acetone. This unexpected peninsula is not present if the branched polymer is replaced by the linear polymer [130]. Additionally, the phase diagram of the system linear polyisoprene + branched polyisoprene + cyclohexane was measured [130]. In this ternary system one miscibility gap starting at the binary subsystem linear polyisoprene + branched polyisoprene occurs. Unfortunately, to the best of our knowledge, such experiments were not performed with hyperbranched polymers.

Figure 14. Experimental (black open squares: *n*-dodecane [131–133]; red open squares: *n*-pentadecane [132–135]; blue open squares: *n*-eicosane [132,133]) and calculated vapour pressures of *n*-alkanes (black line: *n*-dodecane ($\sigma = 3.11513 \times 10^{-10} m$; $\varepsilon/k_B = 109.94 K$); red line: *n*-pentadecane ($\sigma = 3.08592 \times 10^{-10} m$; $\varepsilon/k_B = 111.143 K$); blue line: *n*-eicosane ($\sigma = 3.04986 \times 10^{-10} m$; $\varepsilon/k_B = 112.69 K$). The stars mark the experimental critical points [132,136].



3.5. Compressible LCT

In Section 2.2.2 a version of the LCT of compressible systems is presented. This version can be reformulated as an equation of state for pure components [111,112]. The derived equation of state (Equation (61)) can be used to calculate the thermodynamic properties of a pure component, for

instance the vapour pressure as function of temperature. In Figure 14 the calculated vapour pressures are compared with the experimental ones from literature [131–135] for relatively long chain *n*-alkanes. In this theoretical approach two parameters describing a pure component occur. The first parameter is the length of a cubic cell on the lattice σ and the second one is the interaction energy, ε_{ii} . From Figure 14 the potential of this new equation of state can be seen, because the experimental data were described with a high accuracy, although only two pure component parameters are used.

4. Summary

In summing up the theoretical investigations we can state that the LCT in combination with the Lattice Wertheim approach is a promising tool to calculate the thermodynamic properties of polymer containing systems, especially if hyperbranched polymers are involved. In this way it could be shown, that besides the architecture of the hyperbranched polymer, the influence of functional groups also has to be considered in the theoretical framework.

Acknowledgments

For financial support the authors thank the German Science Foundation (DFG, En 291/7-1) and the Max-Buchner Research Foundation (Nr. 2864). The authors thank the company Perstorp Speciality Chemicals AB for donating the hyperbranched polymer as gift and Johannes Sailer for performing some of the model calculations.

References

- 1. Zou, J.; Shi, W.; Wang, J.; Bo, J. Encapsulation and controlled release of a hydrophobic drug using a novel nanoparticle forming hyperbranched polyester. *Macromol. Biosci.* **2005**, *5*, 662-668.
- 2. Paleos, C.M.; Tsiourvas, D.; Sideratou, Z.; Tziveleka, L.-A. Drug delivery using multifunctional dendrimers and hyperbranched polymers. *Expert Opin. Drug Deliv.* **2010**, *7*, 1387-1398.
- 3. Frey, H.; Haag, R. Dendritic polyglycerol: A new versatile biocompatible material. *Rev. Mol. Biotechnol.* **2002**, *90*, 257-267.
- 4. Svenson, S.; Tomalia, D.A. Dendrimers in biomedical applications—Reflections on the field. *Adv. Drug Deliv. Rev.* **2005**, *57*, 2106-2129.
- Kainthan, R.K.; Gnanamani, M.; Ganguli, M.; Ghosh, T.; Brooks, D.E.; Maiti, S.; Kizhakkedathu, J.N. Blood compatibility of novel water soluble hyperbranched polyglycerol-based multivalent cationic polymers and their interaction with DNA. *Biomaterials* 2006, 27, 5377-5390.
- 6. Reichelt, S.; Eichhorn, K.-J.; Aulich, D.; Hinrichs, K.; Jain, N.; Appelhans, D.; Voit, B. Functionalization of solid surfaces with hyperbranched polyesters to control protein adsorption. *Colloids Surfaces B* **2009**, *69*, 169-177.
- 7. Xue, L.; Dai, S.; Li, Z. Biodegradable shape-memory block co-polymers for fast self-expandable stents. *Biomaterials* **2010**, *31*, 8132-8140.

- 8. Shepherd, J.; Sarker, P.; Rimmer, S.; Swanson, L.; MacNeil, S.; Douglas, I. Hyperbranched poly(NIPAM) polymers modified with antibiotics for the reduction of bacterial burden in infected human tissue engineered skin. *Biomaterials* **2011**, *32*, 258-267.
- 9. Tuchbreiter, L.; Mecking, S. Hydroformylation with dendritic-polymer-stabilized rhodium colloids as catalyst precursors. *Macromol. Chem. Phys.* **2007**, *208*, 1688-1693.
- 10. Zhang, G.; Fan, X.; Kong, J.; Liu, Y.; Xie, Y. Hyperbranched organosilicon polymers. *Prog. Chem.* **2008**, *20*, 326-338.
- Marty, J.-D.; Martinez-Aripe, E.; Mingotaud, A.-F.; Mingotaud, C. Hyperbranched polyamidoamine as stabilizer for catalytically active nanoparticles in water. *J. Colloid Interf. Sci.* 2008, 326, 51-54.
- 12. Tahara, K.; Shimakoshi, H.; Tanaka, A.; Hisaeda, Y. Synthesis, characterization and catalytic function of a B 12-hyperbranched polymer. *Dalton Trans.* **2010**, *39*, 3035-3042.
- 13. Cypryk, M.; Pospiech, P.; Strzelec, K.; Wasikowska, K.; Sobczak, J.W. Soluble polysiloxane-supported palladium catalysts for the Mizoroki-Heck reaction. *J. Mol. Catal. A* **2010**, *319*, 30-38.
- 14. Yin, Y.; Yang, L.; Yoshino, M.; Fang, J.; Tanaka, K.; Kita, H.; Okamoto, K.-I. Synthesis and gas permeation properties of star-like poly(ethylene oxide)s using hyperbranched polyimide as central core. *Polym. J.* **2004**, *36*, 294-302.
- 15. Suda, T.; Yamazaki, K.; Kawakami, H. Syntheses of sulfonated star-hyperbranched polyimides and their proton exchange membrane properties. *J. Power Sour.* **2010**, *195*, 4641-4646.
- 16. Kakimoto, M.-A.; Grunzinger, S.J.; Hayakawa, T. Hyperbranched poly(ether sulfone)s: Preparation and application to ion-exchange membranes. *Polym. J.* **2010**, *42*, 697-705.
- Sterescu, D.M.; Stamatialis, D.F.; Mendes, E.; Kruse, J.; Rätzke, K.; Faupel, F.; Wessling, M. Boltom-modified poly(2,6-dimethyl-1,4-phenylene oxide) gas separation membranes. *Macromolecules* 2007, 40, 5400-5410.
- 18. Wei, X.-Z.; Zhu, L.-P.; Deng, H.-Y.; Xu, Y.-Y.; Zhu, B.-K.; Huang, Z.-M. New type of nanofiltration membrane based on crosslinked hyperbranched polymers. *J. Membr. Sci.* 2008, *323*, 278-287.
- 19. Peter, J.; Kosmala, B.; Bleha, M. Synthesis of hyperbranched copolyimides and their application as selective layers in composite membranes. *Desalination* **2009**, *245*, 516-526.
- 20. Arkas, M.; Tsiourvas, D.; Paleos, C.M. Functional dendritic polymers for the development of hybrid materials for water purification. *Macromol. Mater. Eng.* **2010**, *295*, 883-898.
- 21. Seiler, M. Hyperbranched polymers: Phase behavior and new applications in the field of chemical engineering. *Fluid Phase Equilib.* **2006**, *241*, 155-174.
- 22. Rehim, M.A.; Fahmy, H.M.; Mohamed, Z.E.; Abo-Shosha, M.H.; Ibrahim, N.A. Synthesis, characterisation and utilisation of hyperbranched poly (ester-amide) for the removal of some anionic dyestuffs from their aqueous solutions. *Pigment Resin Technol.* **2010**, *39*, 149-155.
- 23. Chen, Y.Z.; Peng, P.; Guo, Z.X.; Yu, J.; Zhan, M.S. Effect of hyperbranched poly(ester amine) additive on electrospinning of low concentration poly(methyl methacrylate) solutions. *J. Appl. Polym. Sci.* **2010**, *115*, 3687-3696.
- 24. Seiler, M. Dendritic polymers—Interdisciplinary research and emerging applications from unique structural properties. *Chem. Eng. Technol.* **2002**, *25*, 237-253.

- 25. Feng, J.; Li, Y.; Yang, M. Hyperbranched copolymer containing triphenylamine and divinyl bipyridyl units for fluorescent chemosensors. *J. Polym. Sci. Part A* **2009**, *47*, 222-230.
- 26. Hartmann-Thompson, C.; Keeley, D.L.; Rousseau, J.R.; Dvornic, P.R. Fluorescent dendritic polymers and nanostructured coatings for the detection of chemical warfare agents and other analytes. *J. Polym. Sci. Part A* **2009**, *47*, 5101-5115.
- 27. Liu, Y.; Dong, Y.; Jauw, J.; Linman, M.J.; Cheng, Q. Highly sensitive detection of protein toxins by surface plasmon resonance with biotinylation-based inline atom transfer radical polymerization amplification. *Anal. Chem.* **2010**, *82*, 3679-3685.
- 28. Caminade, A.M.; Delavaux-Nicot, B.; Laurent, R.; Majoral J.P. Sensitive sensors based on phosphorus dendrimers. *Curr. Org. Chem.* **2010**, *14*, 500-515.
- 29. Foix, D.; Erber, M.; Voit, B.; Lederer, A.; Ramis, X.; Mantecón, A.; Serra, A. New hyperbranched polyester modified DGEBA thermosets with improved chemical reworkability. *Polym. Degrad. Stab.* **2010**, *95*, 445-452.
- Morell, M.; Erber, M.; Ramis, X.; Ferrando, F.; Voit, B.; Serra, A. New epoxy thermosets modified with hyperbranched poly(ester-amide) of different molecular weight. *Eur. Polym. J.* 2010, 46, 1498-1509.
- 31. Deka, H.; Karak, N. Bio-based hyperbranched polyurethane/clay nanocomposites: Adhesive mechanical and thermal properties. *Polym. Adv. Technol.* **2011**, *22*, 973-980.
- 32. Kim, Y.H.; Webster, O.W. Hyperbranched polyphenylenes. *Macromolecules* 1992, 25, 5561-5572.
- Morgan, S.; Ye, Z.; Subramanian, R.; Zhu, S. Higher-molecular-weight hyperbranched polyethylenes containing crosslinking structures as lubricant viscosity-index improvers. *Polym. Eng. Sci.* 2010, *50*, 911-918.
- 34. Frey, H.; Haag, R.; Dendritic polyglycerol: A new versatile biocompatible material. *Rev. Mol. Biotechnol.* **2002**, *90*, 257-267.
- Kainthan, R.K.; Gnanamani, M.; Ganguli, M.; Ghosh, T.; Brooks, D.E.; Maiti, S.; Kizhakkedathu, J.N. Blood compatibility of novel water soluble hyperbranched polyglycerol-based multivalent cationic polymers and their interaction with DNA. *Biomaterials* 2006, 27, 5377-5390.
- Rossi, N.A.A.; Constantinescu, I.; Kainthan, R.K.; Brooks, D.E.; Scott, M.D.; Kizhakkedathu, J.N. Red blood cell membrane grafting of multi-functional hyperbranched polyglycerols. *Biomaterials* 2010, *31*, 4167-4178.
- Perumal, O.; Khandare, J.; Kolhe, P.; Kannan, S.; Lieh-Lai, M.; Kannan, R.M. Effects of branching architecture and linker on the activity of hyperbranched polymer-drug conjugates. *Bioconjug. Chem.* 2009, 20, 842-846.
- 38. Kumar, K.R.; Brooks, D.E. Comparison of hyperbranched and linear polyglycidol unimolecular reverse micelles as nanoreactors and nanocapsules. *Macromol. Rapid Commun.* **2005**, *26*, 155-159.
- 39. Wang, T.; Wu, Y.; Li, M. Novel hyperbranched poly (amine-ester)-poly (lactide-*co*-glycolide) polymeric micelles as amphotericin B carriers. *Polym. Bull.* **2010**, *65*, 425-442.
- 40. Kurniasih, I.N.; Liang, H.; Rabe, J.P.; Haag, R. Supramolecular aggregates of water soluble dendritic polyglycerol architectures for the solubilization of hydrophobic compounds. *Macromol. Rapid Commun.* **2010**, *31*, 1516-1520.

- 41. Oudshoorn, M.H.M.; Penterman, R.; Rissmann, R.; Bouwstra, J.A.; Broer, D.J.; Hennink, W.E. Preparation and characterization of structured hydrogel microparticles based on cross-linked hyperbranched polyglycerol. *Langmuir* **2007**, *23*, 11819-11825.
- 42. Höbel, S.; Loos, A.; Appelhans, D.; Schwarz, S.; Seidel, J.; Voit, B.; Aigner, A. Maltose- and maltotriose-modified, hyperbranched poly(ethylene imine)s (OM_PEIs): Physicochemical and biological properties of DNA and siRNA complexes. *J. Control. Release* **2011**, *149*, 146-158.
- 43. Zhao, D.; Gong, T.; Zhu, D.; Zhang, Z.; Sun, X. Comprehensive comparison of two new biodegradable gene carriers. *Int. J. Pharm.* **2011**, *413*, 260-270.
- 44. Wang, J.; Xu, T. Facile construction of multivalent targeted drug delivery system from Boltorn[®] series hyperbranched aliphatic polyester and folic acid. *Polym. Adv. Technol.* **2011**, *22*, 763-767.
- 45. Jain, N.K.; Gupta, U. Application of dendrimer-drug complexation in the enhancement of drug solubility and bioavailability. *Expert Opin. Drug Metab. Toxicol.* **2008**, *4*, 1035-1052.
- 46. Paleos, C.M.; Tsiourvas, D.; Sideratou, Z.; Tziveleka, L.A. Drug delivery using multifunctional dendrimers and hyperbranched polymers. *Expert Opin. Drug Deliv.* **2010**, *7*, 1387-1398.
- Kim, W.J.; Bonoiu, A.C.; Hayakawa, T.; Xia, C.; Kakimoto, M.A.; Pudavar, H.E.; Lee, K.S.; Prasad, P.N. Hyperbranched polysiloxysilane nanoparticles: Surface charge control of nonviral gene delivery vectors and nanoprobes. *Int. J. Pharm.* 2009, *376*, 141-52.
- 48. Astruc, D.; Boisselier, E.; Ornelas, C. Dendrimers designed for functions: From physical, photophysical, and supramolecular properties to applications in sensing, catalysis, molecular electronics, photonics, and nanomedicine. *Chem. Rev.* **2010**, *110*, 1857-1959.
- 49. Irfan, M.; Seiler, M. Encapsulation using hyperbranched polymers: From research and technologies to emerging applications. *Ind. Eng. Chem. Res.* **2010**, *49*, 1169-1196.
- 50. Wilms, D.; Stiriba, S.E.; Frey, H. Hyperbranched polyglycerols: From the controlled synthesis of biocompatible polyether polyols to multipurpose applications. *Acc. Chem. Res.* **2010**, *43*, 129-141.
- 51. Wurm, F.; Frey, H. Linear-dendritic block copolymers: The state of the art and exciting perspectives. *Prog. Polym. Sci.* **2011**, *36*, 1-52.
- 52. Zagar, E.; Zigon, M. Aliphatic hyperbranched polyesters based on 2,2-bis(methylol)propionic acid Determination of structure, solution and bulk properties. *Prog. Polym. Sci.* 2011, *36*, 53-88.
- 53. Zeiner, T.; Browarzik, D.; Enders, S. Calculation of the liquid-liquid equilibrium of aqueous solutions of hyperbranched polymers. *Fluid Phase Equilib.* **2009**, *286*, 127-133.
- 54. Zeiner, T.; Schrader, P.; Enders, S.; Browarzik, D. Phase- and interfacial behavior of hyperbranched polymer solutions. *Fluid Phase Equilib.* **2011**, *302*, 321-330.
- 55. Enders, S.; Zeiner, T. Application of Lattice Cluster Theory to the Calculation of Miscibility and Interfacial Behavior of Polymer Containing Systems. In *Polymer Phase Behavior*, Ehlers, T.P., Wilhelm, J.K., Eds.; Nova Science Publishers, Inc.: Hauppauge, NY, USA, 2011.
- 56. Zeiner, T.; Enders, S. Phase-behavior of hyperbranched polymer solutions in mixed solvents. *Chem. Eng. Sci.* **2011**, *66*, 5244-5252.
- 57. Zeiner, T.; Browarzik, C.; Browarzik, D.; Enders, S. Calculation of the liquid-liquid equilibrium of solutions of hyperbranched polymers with the lattice-cluster theory combined with an association model. *J. Chem. Thermodyn.* **2011**, *43*, 1969-1976.
- 58. Zeiner, T.; Puyan, M.J.; Schrader, P.; Browarzik, C.; Enders, S. Phase behavior of hyperbranched polymer in demixed solvent. *Mol. Phys.* **2012**, in press.

- 60. de Loos, T.W.; Poot, W.; Lichtenthaler, R.N. The influence of branching on high-pressure vapor-liquid equilibria in systems of ethylene and polyethylene. *J. Supercrit Fluids* **1995**, *8*, 282-286.
- Eckelt, J.; Samadi, F.; Wurm, F.; Frey, H.; Wolf, B.A. Branched *versus* linear polyisoprene: Flory-Huggins interaction parameters for this solutions in cyclohexane. *Macromol. Chem. Phys.* 2009, 210, 1433-1439.
- 62. Stockmayer, W.H. Theory of molecular size distribution and gel formation in branched-chain polymers. *J. Chem. Phys.* **1943**, *11*, 45-55.
- 63. Granath, K.A. Solution properties of branched dextrans. J. Coll. Sci. 1958, 13, 308-328.
- 64. Kleintjens, L.A.; Koningsveld, R. Liquid-liquid phase separation in multicomponent polymer systems. 18. Effect of short-chain branching. *Macromolecules* **1980**, *13*, 303-310.
- 65. Daoud, M.; Pincus, P.; Stockmayer, W.H.; Witten, T. Phase separation in branched polymer solutions. *Macromolecules* **1983**, *16*, 1833-1839.
- 66. de Gennes, P.G.; Hervet, H. Statistics of starburst polymers. J. Phys. Lett. 1983, 44, 351-358.
- 67. van Hunsel, J.; Balazs, A.C.; Koningsveld, R.; MacKnight, W.J. Effect of sequence distribution on the critical composition difference in copolymer blends. *Macromolecules* **1988**, *21*, 1528-1530.
- 68. Seiler, M. Phase Behavior and New Applications of Hyperbranched Polymers in the Field of Chemical Engineering; VDI Verlag: Düsseldorf, Germany, 2004.
- 69. Kouskoumvekaki, I.A.; Giesen, R.; Michelsen, M.L.; Kontogeorgis, G.M. Free-volume activity coefficient models for dendrimer solutions. *Ind. Eng. Chem. Res.* **2002**, *41*, 4848-4853.
- 70. Oishi, T.; Prausnitz, J.M. Estimation of solvent activities in polymer solutions using a group-contribution method. *Ind. Eng. Chem. Proc. Des. Dev.* **1978**, *17*, 333-339.
- 71. Fredenslund, A. *Vapor-Liquid Equilibria Using UNIFAC, a Group-Contribution Method*; Elsevier: Amsterdam, The Netherlands, 1977.
- 72. Müller, E.A.; Gubbins, K.E. Molecular-based equations of state for associating fluids: A review of SAFT and related approaches. *Ind. Eng. Chem. Res.* **2001**, *40*, 2193-2211.
- 73. Wertheim, M.S. Fluids with highly directional attractive forces. I. Statistical thermodynamics. *J. Stat. Phys.* **1984**, *35*, 19-34.
- 74. Wertheim, M.S. Fluids with highly directional attractive forces. II. Thermodynamic perturbation theory and integral equations. *J. Stat. Phys.* **1984**, *35*, 35-47.
- 75. Wertheim, M.S. Fluids with highly directional attractive forces. III. Multiple attraction sites. *J. Stat. Phys.* **1986**, *42*, 459-476.
- Wertheim, M.S. Fluids with highly directional attractive forces. IV. Equilibrium polymerization. J. Stat. Phys. 1986, 42, 477-492.
- 77. Chapman, W.G.; Gubbins, K.E.; Joslin, C.G.; Gray, C.G. Theory and simulation of associating liquid mixtures. *Fluid Phase Equilib.* **1986**, *29*, 337-346.
- 78. Gross, J.; Sadowski, G. Perturbed-chain SAFT: An equation of state based on a perturbation theory for chain molecules. *Ind. Eng. Chem. Res.* **2001**, *40*, 1244-1260.

- 79. Kozłowska, M.K.; Jürgens, B.F.; Schacht, C.S.; Gross, J.; de Loos, T.W. Phase behavior of hyperbranched polymer systems: Experiments and application of the perturbed-chain polar SAFT equation of state. *J. Phys. Chem. B* **2009**, *113*, 1022-1029.
- Blas, F.J.; Vega, L.F. Thermodynamic properties and phase equilibria of branched chain fluids using first- and second-order Wertheim's thermodynamic perturbation theory. *J. Chem. Phys.* 2001, doi: 10.1063/1.1388544.
- 81. Tompa, H. Polymer Solutions; Butterworth: London, UK, 1956.
- 82. Kamide, K. *Thermodynamics of Polymer Solutions*; Elsevier: Amsterdam, The Netherlands, 1990.
- 83. Koningsveld, R.; Stockmayer, W.H.; Nies, E. *Polymer Phase Diagrams*; Oxford University Press: Oxford, UK, 2001.
- 84. Flory, P.J. Principles of Polymer Chemistry; Cornell University Press: Ithaca, NY, USA, 1953.
- 85. Huggins, M.L. Theory of solutions of high polymers. J. Am. Chem. Soc. 1942, 64, 1712-1719.
- 86. Huggins, M.L. *Physical Chemistry of High Polymers*; Cornell University Press: Ithaca, NY, USA, 1953.
- 87. Nemirovsky, A.M.; Bawendi, M.G.; Freed, K.F. Lattice models of polymer solutions: Monomers occupying several lattice sites. *J. Chem. Phys.* **1987**, doi: 10.1063/1.453320.
- 88. Freed, K.F.; Bawendi, M.G. Lattice theories of polymeric fluids. J. Phys. Chem. 1989, 93, 2194-2203.
- Dudowicz, J.; Freed, K.F. Effect of monomer structure and compressibility on the properties of multi-component polymer blends and solutions: 1. Lattice cluster theory of compressible systems. *Macromolecules* 1991, 24, 5076-5095.
- Dudowicz, J.; Freed, M.S.; Freed, K.F. Effect of monomer structure and compressibility on the properties of multi-component polymer blends and solutions. 2. Application to binary blends. *Macromolecules* 1991, 24, 5096-5111.
- Dudowicz, J.; Freed, K.F. Effect of monomer structure and compressibility on the properties of multi-component polymer blends and solutions. 3. Application to deuterated polystyrene [PS(D)]poly(vinyl methyl ether) (PVME) blends. *Macromolecules* 1991, 24, 5112-5123.
- 92. Dudowicz, J.; Freed, K.F.; Madden, W.G. Role of molecular structure on the thermodynamic properties of melts, blends, and concentrated polymer solutions: Comparison of Monte Carlo simulations with the cluster theory for the lattice model. *Macromolecules* **1990**, *23*, 4803-4819.
- 93. Jang, J.G.; Bae, Y.C. Phase behaviors of hyperbranched polymer solutions. *Polymer* **1999**, *40*, 6761-6768.
- 94. Jang, J.G.; Bae, Y.C. Phase behavior of hyperbranched polymer solutions with specific interactions. J. Chem. Phys. 2001, doi: 10.1063/1.1329647.
- 95. Yang, J.; Peng, C.; Liu, H.; Hu, Y.; Jiang, J. A generic molecular thermodynamics model for linear and branched polymer solutions in a lattice. *Fluid Phase Equilib.* **2006**, *244*, 188-192.
- 96. Hu, Y.; Ying, X.; Wu, D.T.; Prausnitz, J.M. Molecular thermodynamics of polymer solutions. *Fluid Phase Equilib.* **1993**, *83*, 289-300.
- 97. Newkome, G.R.; Moorefield, C.N. Stiff Dendritic Macromolecules Based on Phenylacetylenes. In *Advances in Dendritic Macromolecules*; Newkome, G.R., Ed.; JAI Press: Greenwich, CT, USA, 1994; Volume 1, pp. 1-23.

- 98. Economou, I.G.; Donohue, M.D. Chemical, quasi-chemical and perturbation theories for associating fluids. *AIChE J.* **1991**, *37*, 1875-1894.
- 99. Mayer, J.E.; Mayer, M.G. Statistical Mechanics; John Wiley & Sons Inc.: Hoboken, NJ, USA, 1940.
- 100. Constantine, T. Thermodynamic analysis of the mutual solubilities of normal alkanes and water. *Fluid Phase Equilib.* **1999**, *156*, 21-33.
- 101. Schnell, M.; Stryuk, S.; Wolf, B.A. Liquid/Liquid demixing in the system n-hexane/narrowly distributed linear polyethylene. *Ind. Eng. Chem. Res.* **2004**, *43*, 2852-2859.
- 102. Gibbs, J.W. *The Collected Works of J. Willard Gibbs*; Yale University Press: New Haven, CT, USA, 1957.
- 103. Reed, T.M.; Gubbins, K.E. *Applied Statistical Mechanics*; McGraw-Hill Inc.: New York, NY, USA, 1973.
- 104. Jones, G.H.; Pfeffer, W.; Raoult, F.M.; van't Hoff, J.H.; Arrhenius, S. The Modern Theory of Solution: Memoirs by Pfeffer, van't Hoff, Arrhenius, and Raoult; Harper: New York, NY, USA, London, UK, 1899.
- 105. Freed, K.F. New lattice model for interacting, avoiding polymers with controlled length distribution. J. Phys. A **1985**, 18, 871-877.
- 106. de Gennes, P.G. Exponents for the excluded volume problem as derived by the Wilson method. *Phys. Lett. A* **1972**, *38*, 339-340.
- des Cloizeaux, J. The Lagrangian theory of polymer solutions at intermediate concentrations. J. Phys. 1975, 36, 281-291.
- 108. Pesci, A.I.; Freed, K.F. Lattice models of polymer fluids: Monomers occupying several lattice sites. II. Interaction energies. *J. Chem. Phys.* **1989**, *90*, 2003-2016.
- 109. Freed, K.F.; Dudowicz, J. Influence of monomer molecular structure on the miscibility of polymer blends. *Adv. Polym. Sci.* 2005, *183*, 63-126.
- 110. Dudowicz, J.; Freed, K.F.; Douglas, J.F. Modification of the phase stability of polymer blends by diblock coplymer additives. *Macromolecules* **1995**, *28*, 2276-2287.
- 111. Langenbach, K. Application of Lattice Cluster Theory to Compressible Systems. Ph.D. thesis, TU Berlin, Berlin, Germany; in preparation.
- 112. Langenbach, K.; Enders, S. Development of an EOS based on lattice cluster theory. *Fluid Phase Eqilib.* to be submitted for publication.
- 113. Nemirovsky, A.M.; Dudowicz, J.; Freed, K.F. Dense self-interacting lattice trees with specified topologies: From light to dense branching. *Phys. Rev. A* **1992**, *45*, 7111-7127.
- 114. Žagar, E.; Grdadolnik, J. An infrared spectroscopic study of H-bond network in hyperbranched polyester polyol. *J. Mol. Struct.* **2003**, *658*, 143-152.
- 115. Turky, G.; Shaaban, S.S.; Schöenhals, A. Broadband dielectric spectroscopy on the molecular dynamics in different generations of hyperbranched polyester. J. Appl. Polym. Sci. 2009, 113, 2477-2484.
- 116. Tanis, I.; Karatasos, K. Local dynamics and hydrogen bonding in hyperbranched aliphatic polyesters. *Macromolecules* **2009**, *42*, 9581-9591.
- 117. Morita, T.; Hiroike, K. A new approach to the theory of classical fluids. III. *Prog. Theor. Phys.* **1961**, *25*, 537-578.

- 118. Stell, G. Cluster Expansions for Classical Systems in Equilibrium. In *The Equilibrium Theory of Classical Fluids*; Frisch, H.L., Lebowitz, J.L., Eds.; Frontiers in Physics; W. A. Benjamin: New York, NY, USA, 1964.
- 119. Kirkwood, J.G.; Buff, F.P. The statistical mechanical theory of solutions. I. J. Chem. Phys. 1951, doi: 10.1063/1.1748352.
- 120. Nies, E.; Li, T.; Berghmans, H.; Heenan, R.K.; King, S.M. Upper critical solution temperature phase behavior, composition fluctuations, and complex formation in poly (Vinyl methyl ether)/D₂O solutions: Small-Angle neutron-scattering experiments and wertheim lattice thermodynamic perturbation theory predictions. *J. Phys. Chem. B* **2006**, *110*, 5321-5329.
- 121. Nies, E.; Ramzi, A.; Berghmans, H.; Li, T.; Heenan, R.K.; King, S.M. Composition fluctuations, phase behavior, and complex formation in poly(vinyl methyl ether)/D₂O investigated by small-angle neutron scattering. *Macromolecules* 2005, *38*, 915-924.
- 122. Langenbach, K.; Enders, S. Cross-Association of Multicomponent Systems. In *Process Engineering and Chemical Plant Design*; Wozny, G., Hady, L., Eds.; Universitätsverlag der TU Berlin: Berlin, Germany, 2011.
- Grenner, A.; Kontogeorgis, G.M.; von Solms, N.; Michelsen, M.L. Application of PC-SAFT to glycol containing systems—PC-SAFT towards a predictive approach. *Fluid Phase Equilib.* 2007, 261, 248-257.
- 124. Saeki, S. Combinatory entropy in complex polymer solutions. Polymer 2000, 41, 8331-8338.
- 125. Arya, G.; A.Z. Panagiotopoulos, A.Z. Impact of branching on the phase behavior of polymers. *Macromolecules* **2005**, *38*, 10596-10604.
- 126. Alessi, M.L.; Bittner, K.C.; Greer, S.C. Eight-arm star polystyrene in methylcyclohexane: Cloud-point curves. *J. Polym. Sci. Part B* 2004, *42*, 129-145.
- 127. Yokoyama, H.; Takano, A.; Okado, M.; Nose, T. Phase diagram of star-shaped polystyrene/cyclohexane system: Location of critical point and profile of coexistence curve. *Polymer* **1991**, *32*, 3218-3224.
- 128. Domańska, U.; Paduszyński, K.; ZoŁek-Tryznowska, Z. Liquid-liquid phase equilibria of binary systems containing hyperbranched polymer B-U3000: Experimental study and modeling in terms of lattice cluster theory. *J. Chem. Eng. Data* **2010**, *55*, 3842-3846.
- 129. Stephenson, R.; Stuart, J. Mutual binary solubilities: Water-alcohols and water-esters. J. Chem. Eng. Data 1986, 31, 56-70.
- 130. Samadi, F.; Eckelt, J.; Wolf, B.A.; Lopez-Villanueva, F.J.; Frey, H. Branched *versus* linear polyisoprene: Fractionation and phase behavior. *Eur. Polym. J.* **2007**, *43*, 4236-4243.
- 131. Francis, A.W. Pressure-temperature-liquid density relations of pure hydrocarbons. *Ind. Eng. Chem.* **1957**, *49*, 1779-1786.
- 132. Vargaftik, N.B. *Tables on the Thermophysical Properties of Liquids and Gases*; Hemisphere Publishing Corporation: Washington, DC, USA, 1975.
- 133. Green, D.W.; Perry, R.H. Perry's Chemical Engineers' Handbook; McGraw-Hill Professional: New York, NY, USA, 1997.
- 134. Stull, D.R. Vapor pressure of pure substances. Organic and inorganic compounds. *Ind. Eng. Chem.* **1947**, *39*, 517-540.

- 135. Camin, D.L.; Rossini, F.D. Physical properties of fourteen API research hydrocarbons, C₉ to C₁₅. *J. Phys. Chem.* **1955**, *59*, 1173-1179.
- 136. Ambrose, D.; Tsonopoulos, C. Vapor-liquid critical properties of elements and compounds. 2. Normal Alkanes. J. Chem. Eng. Data 1995, 40, 531-546.

 \bigcirc 2012 by the authors; licensee MDPI, Basel, Switzerland. This article is an open access article distributed under the terms and conditions of the Creative Commons Attribution license (http://creativecommons.org/licenses/by/3.0/).